# The SUMO E3 Ligase MdSIZ1 Targets MdbHLH104 to Regulate Plasma Membrane H$^+$-ATPase Activity and Iron Homeostasis[1][OPEN]

**Li-Jie Zhou,[a] Chun-Ling Zhang,[a] Rui-Fen Zhang,[a,b] Gui-Luan Wang,[a] Yuan-Yuan Li,[a] and Yu-Jin Hao[a,2,3]**

[a]State Key Laboratory of Crop Biology, National Research Center for Apple Engineering and Technology, College of Horticulture Science and Engineering, Shandong Agricultural University, Tai-An, Shandong 271018, China
[b]Qingdao Academy of Agricultural Science, Qing-Dao, Shandong 266100, China

**ORCID ID: 0000-0001-7258-3792 (Y.-J.H.)**

SIZ1 (a SIZ/PIAS-type SUMO E3 ligase)-mediated small ubiquitin-like modifier (SUMO) modification of target proteins is important for various biological processes related to abiotic stress resistance in plants; however, little is known about its role in resistance toward iron (Fe) deficiency. Here, the SUMO E3 ligase MdSIZ1 was shown to be involved in the plasma membrane (PM) H$^+$-ATPase-mediated response to Fe deficiency. Subsequently, a basic helix-loop-helix transcription factor, MdbHLH104 (a homolog of Arabidopsis bHLH104 in apple), which acts as a key component in regulating PM H$^+$-ATPase-mediated rhizosphere acidification and Fe uptake in apples (*Malus domestica*), was identified as a direct target of MdSIZ1. MdSIZ1 directly sumoylated MdbHLH104 both in vitro and in vivo, especially under conditions of Fe deficiency, and this sumoylation was required for MdbHLH104 protein stability. Double substitution of K139R and K153R in MdbHLH104 blocked MdSIZ1-mediated sumoylation in vitro and in vivo, indicating that the K139 and K153 residues were the principal sites of SUMO conjugation. Moreover, the transcript level of the *MdSIZ1* gene was substantially induced following Fe deficiency. *MdSIZ1* overexpression exerted a positive influence on PM H$^+$-ATPase-mediated rhizosphere acidification and Fe uptake. Our findings reveal an important role for sumoylation in the regulation of PM H$^+$-ATPase-mediated rhizosphere acidification and Fe uptake during Fe deficiency in plants.

Iron (Fe) is one of the most important micronutrients in both plants and humans. In plants, Fe acts as a cofactor for a wide variety of proteins participating in many cellular functions, such as hormone biosynthesis, photosynthesis, nitrogen fixation, and mitochondrial respiration (Hänsch and Mendel, 2009). Moreover, Fe deficiency is one of the major causes of anemia in humans, and a diet rich in plants can be a major source of Fe. Importantly, even when the Fe content in the topsoil is high, Fe deficiency in plants is still common, as it generally exists as insoluble ferric hydroxides in the soil. As such, low-Fe stress can be a major factor limiting crop yield and quality.

To cope with conditions of Fe deficiency, angiosperms have evolved two distinct strategies. In dicotyledonous plants and nongraminaceous monocot species, the extrusion of protons mediated by plasma membrane (PM) H$^+$-ATPases acidifies the soil to make Fe(III) more soluble. Subsequently, FRO2 (FERRIC REDUCTASE OXIDASE2) converts $Fe^{3+}$ to $Fe^{2+}$, which is then transported into the roots via IRT1 (IRON REGULATED TRANSPORTER1; Curie and Briat, 2003; Hell and Stephan, 2003; Walker and Connolly, 2008; Hindt and Guerinot, 2012). In contrast, graminaceous plants release phytosiderophores to chelate Fe from the soil. The resultant chelated complexes are then imported into root epidermal cells via a specific transport system (Mori, 1999; Kobayashi et al., 2010).

Transcriptional regulation is one of the most common ways to regulate the function of genes involved in Fe homeostasis under Fe-deficient conditions. A number of transcription factors (TFs), such as the basic helix-loop-helix (bHLH) TFs, have been identified to positively regulate the Fe deficiency response (Kobayashi and Nishizawa, 2012). The first subgroup Ib bHLH protein characterized from plants was FER in tomato (*Solanum lycopersicum*; Ling et al., 2002). Its Arabidopsis (*Arabidopsis thaliana*) ortholog FIT (FER-LIKE IRON DEFICIENCY-INDUCED TRANSCRIPTION FACTOR) controls ferric reduction response and Fe transport into the plant root by directly regulating the transcription of the *FRO2* and *IRT1* genes under the conditions of Fe deficiency (Colangelo and Guerinot, 2004; Yuan, 2005; Yuan et al., 2008). What's more, FIT can

[1]This work was supported by grants from the National Natural Science Foundation of China (31430074 and 31772275), the Ministry of Education of China (IRT15R42), the Ministry of Agriculture of China (CARS-28) and Shandong Province (SDAIT-06-03).

[2]Author for contact: haoyujin@sdau.edu.cn.
[3]Senior author.
The author responsible for distribution of materials integral to the findings presented in this article in accordance with the policy described in the Instructions for Authors (www.plantphysiol.org) is: Yu-Jin Hao (haoyujin@sdau.edu.cn).

Y.-J.H. and L.-J.Z. conceived and designed the experiments; L.-J.Z. performed most of the experiments; C.-L.Z., R.-F.Z., G.-L.W. and Y.-Y.L provided technical assistance; L.-J.Z. and Y.-J.H. analyzed the data and wrote the manuscript.
[OPEN]Articles can be viewed without a subscription.
www.plantphysiol.org/cgi/doi/10.1104/pp.18.00289

 

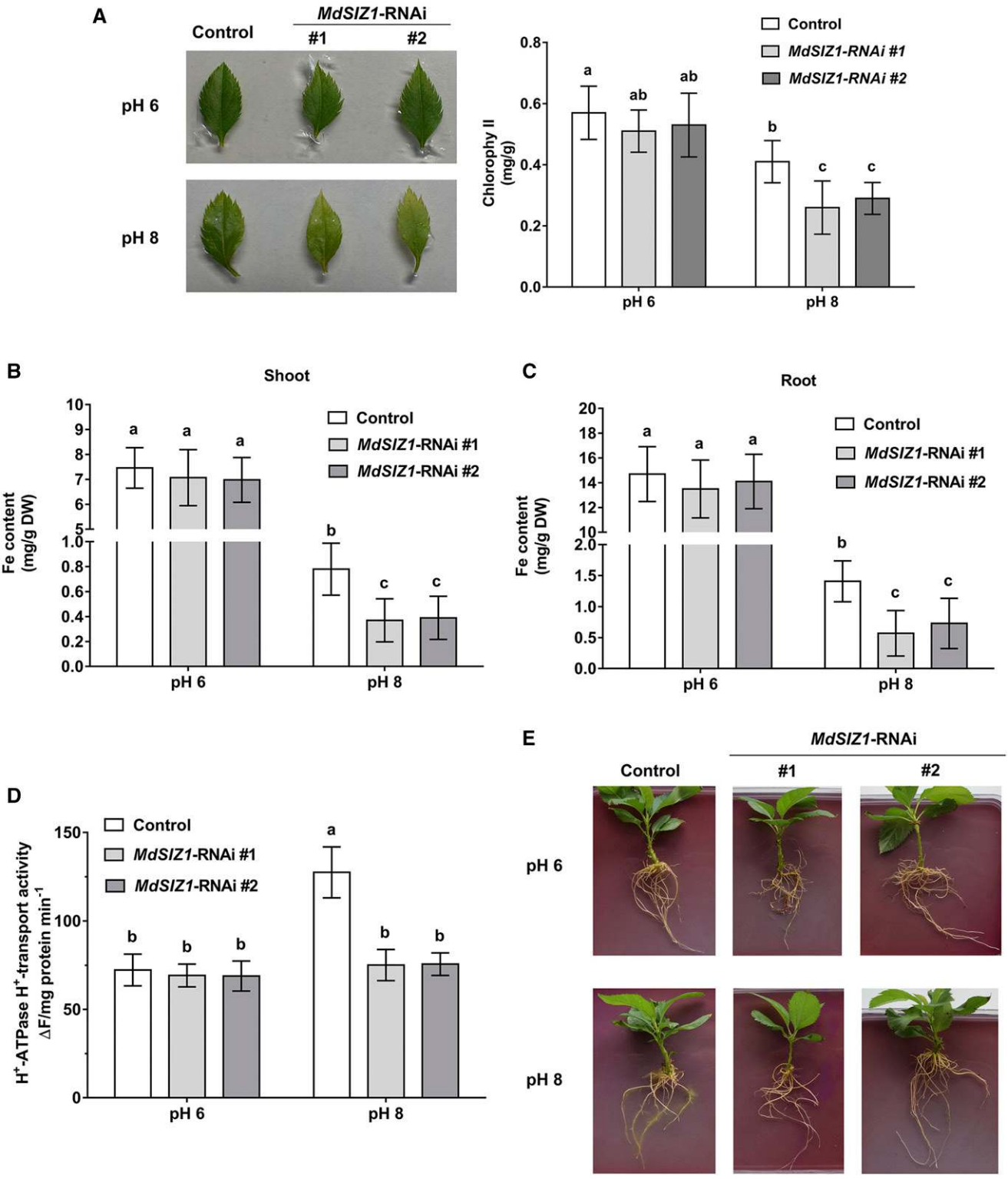


**Figure 1.** *MdSIZ1* knockdown increases the sensitivity of apple to Fe deficiency. After 28 d of subculture, 'Gala' apple cultures were infected with *Agrobacterium tumefaciens* containing empty vector (control) or *MdSIZ1*-RNAi silencing vector to induce hair root. Thereinto, the infection of *MdSIZ1*-RNAi was carried out twice, and each batch of 15 cultures was denoted as #1 and #2, respectively. Each batch of 15 cultures were randomly divided into five groups to conduct different experiments. Biological replicates were carried out with the three cultures in each group to calculate the SD, which are indicated by error bars. Different letter codes have significant difference ($P < 0.01$, ANOVA, Tukey correction). A, The appearance of chlorosis and total chlorophyll contents in young leaves of control and *MdSIZ1*-RNAi chimeric plants in normal (pH 6) or alkaline (pH 8) medium for 20 d.

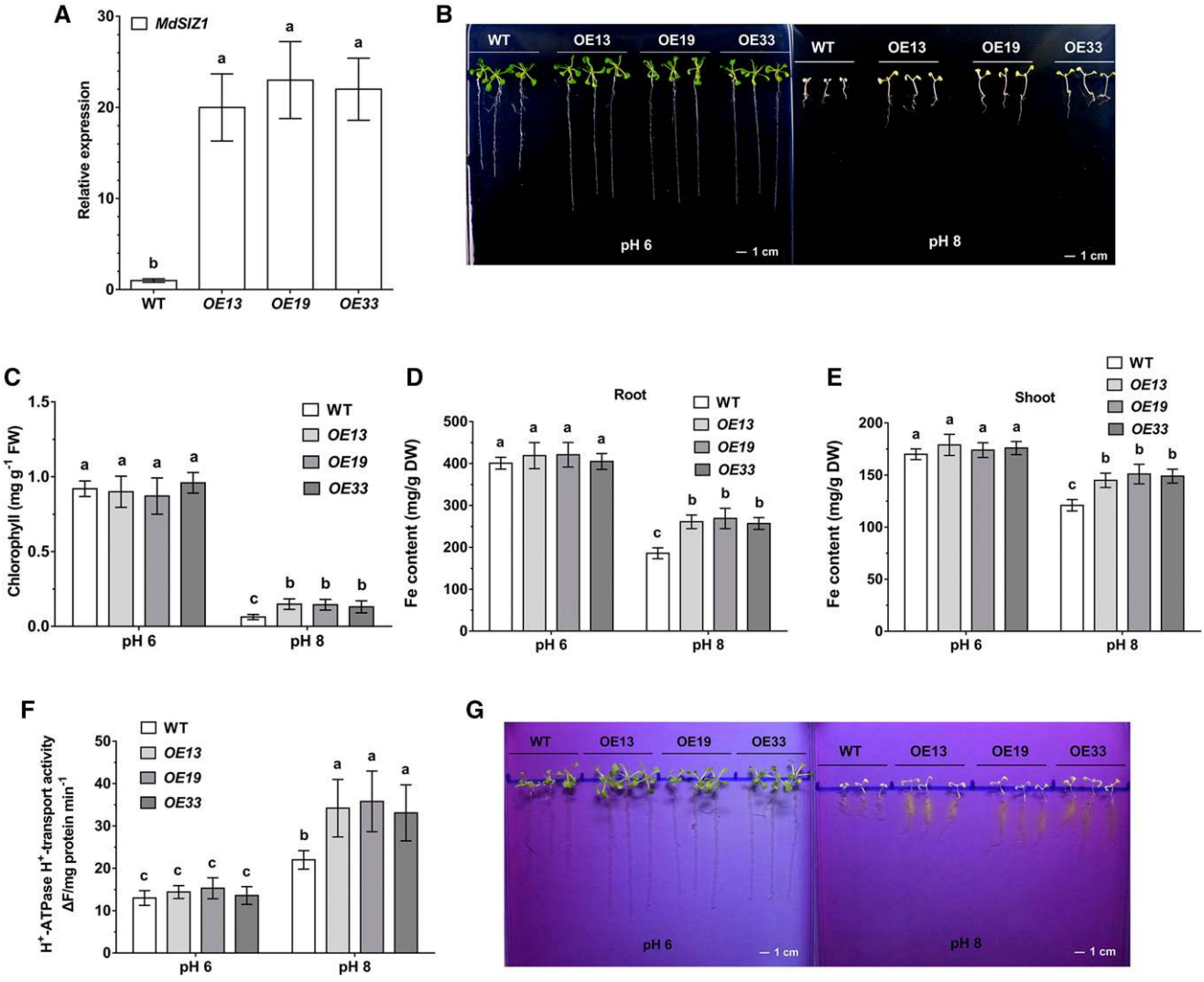


**Figure 2.** Heterologous expression of *MdSIZ1* enhances Fe-deficient stress tolerance in Arabidopsis seedlings. A, *MdSIZ1* expression in wild-type (WT) and transgenic Arabidopsis seedlings. RNA was prepared from seedlings. B, Phenotypes of the wild type and *MdSIZ1* overexpression lines grown for 14 d on normal (pH 6) or alkaline (pH 8) media. Scale bars, 1 cm. C, Chlorophyll contents in 14-d-old wild type and the *MdSIZ1* overexpression lines. FW, Fresh weight. D and E, Fe contents in 14-d-old roots and shoots of plants. DW, Dry weight. F, PM $H^+$-ATPase $H^+$-transport activity in 14-d-old wild type and the *MdSIZ1* overexpression lines. G, Rhizosphere acidification in 14-d-old wild-type and *MdSIZ1* overexpression lines. Acidification is indicated by a yellow color around the roots. Scale bars, 1 cm. Error bars indicate the SD for three biological replicates in which the experiments were carried out three times using the seedlings of each line. Samples denoted by different letters are significantly different ($P < 0.01$, ANOVA, Tukey correction).

form a heterodimer with other members of the Ib subgroup of bHLH TFs, including bHLH38/39/100/101, to constitutively activate *IRT1* and *FRO2* (Yuan et al., 2008; Wang et al., 2013). In addition to those of the Ib subgroup, IVc subgroup bHLH TFs also influence Fe homeostasis under Fe-deficient conditions. For example, the PYE bHLH protein was up-regulated by Fe-deficient conditions. The Fe transport-related genes *NICOTIANAMINE SYNTHASE4*, *ZINC-INDUCED FACILITATOR1*, and *FRO3* were up-regulated in the *pye-1* mutant under Fe-deficient conditions, suggesting PYE functions as a negative regulator of the Fe

**Figure 1.** (*Continued.*)
B and C, Total Fe content in shoots and roots of control and *MdSIZ1*-RNAi chimeric plants grown in normal (pH 6) or alkaline (pH 8) medium for 20 d. DW, Dry weight. D, PM $H^+$-ATPase $H^+$-transport activity in control and *MdSIZ1*-RNAi chimeric plants grown in normal (pH 6) or alkaline (pH 8) medium for 7 d. E, The rhizosphere acidification of control and *MdSIZ1*-RNAi chimeric plants grown in normal (pH 6) or alkaline (pH 8) medium for 7 d. The yellow color around the roots stained with bromocresol purple indicates rhizosphere acidification.

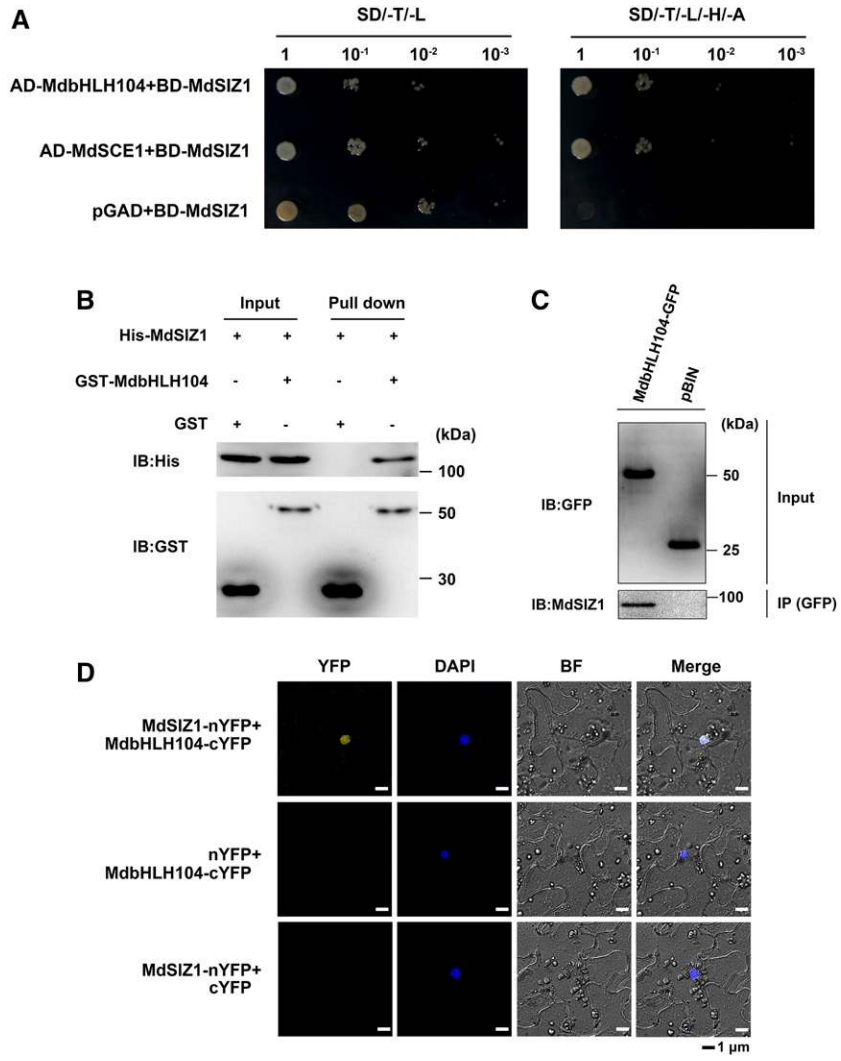


**Figure 3.** MdSIZ1 Interacts with MdbHLH104 Both In Vitro and In Vivo. A, Interaction between MdSIZ1 and MdbHLH104 in yeast cells. Dilution series of yeast cells coexpressing the indicated proteins were grown for 2 d at 28°C. SD/−T/−L indicates Leu and Trp dropout synthetic dropout medium; SD/−T/−L/−H/−A indicates Leu, Trp, His, and Ade dropout synthetic dropout medium. AD-MdSCE1 (SUMO E2 conjugating enzyme1) + BD-MdSIZ1 and AD (pGAD empty vector) + BD-MdSIZ1 were used as positive and negative controls, respectively. B, Interaction between MdSIZ1 and MdbHLH104 in an in vitro pull-down assay. Recombinant GST-MdbHLH104 fusion and His-MdSIZ1 fusion proteins were mixed in equal volume, and following incubation proteins were purified with a GST column. In vitro-translated GST protein was used as a negative control. "Input" indicates protein mixtures before the experiments, "Pull-down" indicates purified protein mixture. "+" indicates presence, and "−" indicates absence. IB, immunoblot. C, Interaction between MdSIZ1 and MdbHLH104 in a Co-IP assay. MdbHLH104-GFP and GFP proteins were IPed from the *35S:MdbHLH104-GFP* and *35S:GFP* (pBIN) transgenic apple plants with anti-GFP antibodies. MdbHLH104-GFP proteins and GFP proteins in whole-cell lysates (Input) and MdSIZ1 proteins in the pellet fraction (IP) were detected via immunoblot analysis with anti-GFP and anti-MdSIZ1 antibodies, respectively. IB, immunoblot. D, Interaction between MdSIZ1 and MdbHLH104 in a BiFC assay. The MdSIZ1-nYFP and MdbHLH104-cYFP constructs were coexpressed transiently in tobacco leaves and visualized by fluorescence microscopy. DAPI was used to stain the nuclei. YFP, Yellow fluorescent protein; BF, bright field. Scale bars, 1 μm.

deficiency response (Long et al., 2010). Most recently, Zhang et al. (2015) reported that the IVc subgroup bHLH TFs bHLH104 and bHLH105 formed a heterodimer to positively regulate Fe deficiency response by directly activating the transcription of genes encoding the Ib bHLH TFs bHLH38/39/100/101. What's more, AtbHLH104 also regulates the acidification of rhizospheres under Fe-deficient conditions (Zhang et al., 2015).

Plant PM $H^+$-ATPases are composed of a series of proton pumps that are driven by ATP hydrolysis, providing an energy source to transport nutrients into plant cells by generating electrochemical gradients (Haruta and Sussman, 2012). In Fe deficiency responses,

PM H+-ATPases play a crucial role in the first step toward improving the plant's ability to acquire Fe from the soil in response to low Fe, especially in dicotyledonous plants. In Arabidopsis, there are a total of 11 *AHA* genes that encode functional PM H+-ATPase proteins that respond to various environmental stimuli (Palmgren, 2001). Among them, *AHA2*, *AHA3*, *AHA4*, and *AHA7* are transcriptionally inducible by low-Fe stress, and AHA2 is involved in rhizosphere acidification (Santi and Schmidt, 2009). Among the 18 apple (*Malus domestica*) MdAHAs, MdAHA1, MdAHA3, MdAHA7, MdAHA8, MdAHA9, MdAHA11, and MdAHA12 are closely related to AtAHA2, and MdAHA8 plays an important role in Fe homeostasis (Zhao et al., 2016a).

In plants, PM H+-ATPases are regulated by various factors at different levels. At the posttranslational level, PM H+-ATPases can be activated by phosphorylation. For example, PM H+-ATPase AHA2 in Arabidopsis, which is mainly responsible for rhizosphere acidification under iron deficiency, is phosphorylated at Ser-931 in the C-terminal regulatory domain by protein kinase PKS5. The phosphorylation of this site inhibits the interaction between AHA2 and an activating 14-3-3 protein, resulting in inhibited PM H+-ATPase activity (Fuglsang et al., 2007). In addition, SAUR proteins, which are positive effectors of cell expansion, are rapidly induced by auxin and serve to negatively regulate PP2C-D phosphatases. Subsequently, the decreased PP2C-D activity alters phosphorylation of PM H+-ATPases, which promotes cell expansion through an acid growth mechanism (Spartz et al., 2014). Moreover, aluminum stress promotes phosphorylation of PM H+-ATPases and their binding with 14-3-3 proteins in black soybeans (*Glycinemax merr*; Guo et al., 2013).

In addition to posttranslational modification, transcriptional regulation is a common manner by which cells modulate the activity of PM H+-ATPases. Many TFs are found to regulate PM H+-ATPase in plants. For example, the expression and activity of AtAHA2 are positively regulated by GsERF71, a TF of the AP2/ERF family from wild soybean (*Gly soja*), in response to alkaline stress (Yu et al., 2017). Additionally, bHLH TFs associated with Fe homeostasis are also involved in the regulation of PM H+-ATPase gene transcription. For example, the chrysanthemum (*Chrysanthemum morifolium*) bHLH TF CmbHLH1 enhances the activity of H+-ATPase CmHA to promote rhizosphere acidification and Fe homeostasis (Zhao et al., 2014). Recently, it was found that the IVc subgroup bHLH TF MdbHLH104, the apple homolog of AtbHLH104, directly binds to the promoter of the *MdAHA8* gene to activate PM H+-ATPase activity in response to Fe deficiency (Zhao et al., 2016a).

Furthermore, regulators that act upstream of these TFs to modulate PM H+-ATPase activity and Fe homeostasis have also been identified. MdBT1 and MdBT2 belong to the BTB/TAZ family of proteins. They recruit the $MdBTs^{MdCUL3}$ E3 ligase complex to target MdbHLH104 for ubiquitination to promote its degradation via a 26S proteasome pathway (Zhao et al., 2016b). Similarly, an E3 ubiquitin ligase BTS interacts with bHLH104 and ILR3 (also called bHLH105) and negatively regulates Fe absorption (Selote et al., 2015; Zhang et al., 2015). Degradation of TFs that positively regulate PM H+-ATPase activity and Fe uptake protects plants from injury caused by generation of Fe overload-associated reactive oxygen species (ROS; Zhao et al., 2016b).

The conjugation of small ubiquitin-like modifier (SUMO) to target proteins is another important posttranslational modification that, in most cases, serves to antagonize the effects of ubiquitination of target proteins (Ulrich, 2005). In plants, sumoylation is an important posttranslational modification of substrate proteins that involves three enzymatic steps catalyzed by a single E1 SUMO-activating enzyme (SAE1 and SAE2 as its subunits), a single E2-conjugating enzyme, SCE1, and two classes of E3 ligase enzymes, including MMS21 and SIZ1 (Miura et al., 2005; Huang et al., 2009; Ishida et al., 2012; Novatchkova et al., 2012). SUMO modification of substrate proteins mediated by SIZ1 mediates various biological processes related to nutrient acquisition and abiotic stresses. For example, in Arabidopsis, SIZ1 positively controls nitrogen assimilation by directly sumoylating the nitrate reductases NIA1 and NIA2 (Park et al., 2011); Heterologous expression of *OsSIZ1*, a rice (*Oryza sativa*) SUMO E3 ligase, enhances broad abiotic stress tolerance and mineral uptake in transgenic creeping bentgrass (*Agrostis stolonifera*; Li et al., 2013). In Arabidopsis, SIZ1 targets PHR1 and ABI5 proteins for SUMO modification to regulate the phosphate deficiency response and ABA signaling (Miura et al., 2005, 2009). Interestingly, PM H+-ATPases are involved in many abiotic stress responses that are associated with SIZ1-mediated sumoylation, such as the phosphate starvation response and ABA response (Yuan et al., 2017). However, it is largely unknown if and/or how SIZ1-mediated sumoylation regulates PM H+-ATPases in response to abiotic stresses, such as Fe deficiency.

In this study, MdbHLH104, an upstream regulator of the PM H+-ATPase gene *MdAHA8* was identified via yeast two-hybrid as an MdSIZ1-interacting protein. MdSIZ1 was further characterized as having functions in sumoylation and affecting the stability of the MdbHLH104 protein. Finally, the molecular mechanism by which MdSIZ1 regulates PM H+-ATPase-mediated rhizosphere acidification during Fe homeostasis is summarized and discussed.

## RESULTS

### The SUMO E3 Ligase MdSIZ1 Is Involved in the PM H+-ATPase-Mediated Response to Fe Deficiency

To examine if MdSIZ1 is involved in response to Fe deficiency, reverse transcription quantitative PCR (RT-qPCR) was conducted. Our analysis showed that

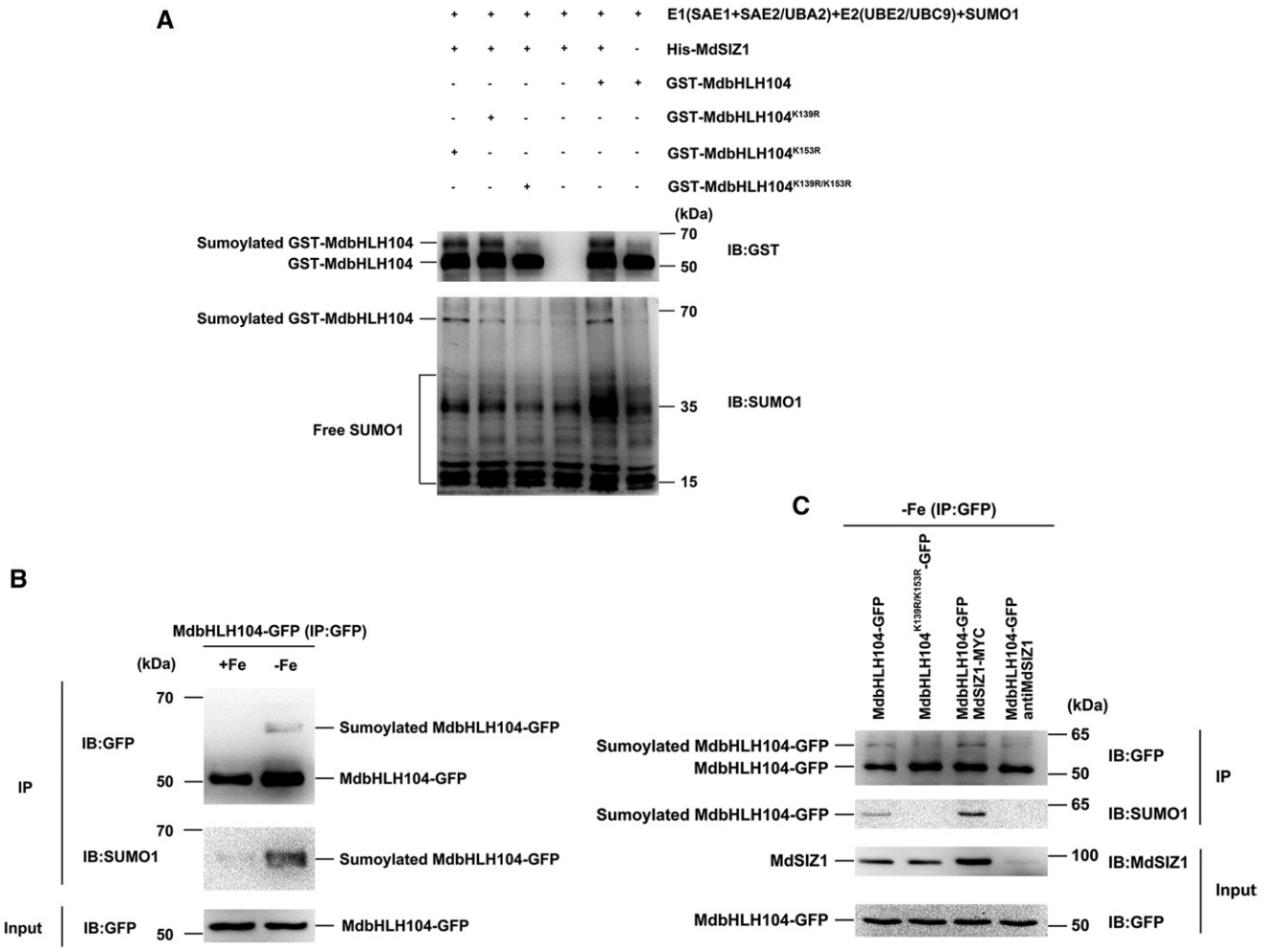


**Figure 4.** MdSIZ1 directly sumoylates MdbHLH104 proteins at residues K139 and K153 under conditions of Fe deficiency. A. SUMO1-MdbHLH104 conjugate detection in vitro. Free SUMO (including monomeric and polymeric forms) are indicated by a brace. IB: Immunoblot. B. SUMO modification of MdbHLH104 under Fe deficiency. The proteins were IPed from *35S:MdbHLH104-GFP* transgenic apple plants using anti-GFP antibodies after treatment with Fe-sufficient or deficient conditions for 1 h. MdbHLH104-GFP proteins in whole-cell lysates prior to treatment (Input) and in the pellet fraction (IP), or sumoylated MdbHLH104 proteins in the pellet fraction (IP), were detected via immunoblot analysis with anti-GFP and anti-SUMO1 antibodies, respectively. IB: Immunoblot. C. Sumoylation of wild type and mutant MdbHLH104 proteins under conditions of Fe deficiency in vivo. The proteins from different transgenic calli, specifically *MdbHLH104-GFP*, *MdbHLH104$^{K139R/K153R}$-GFP*, *MdbHLH104-GFP/MdSIZ1-MYC*, and *MdbHLH104-GFP/antiMdSIZ1*, were IPed with anti-GFP antibodies after treatment at Fe-deficient conditions for 1 h. MdbHLH104-GFP proteins in whole-cell lysates prior to treatment (Input) and in the pellet fraction (IP) or sumoylated MdbHLH104 proteins in the pellet fraction (IP) were detected via immunoblot analysis with anti-GFP and anti-SUMO1 antibodies, respectively. MdSIZ1 proteins in whole-cell lysates prior to treatment (Input) were detected by anti-MdSIZ1 antibodies to confirm the transgenic calli. IB, immunoblot.

transcript levels of *MdSIZ1* were elevated by Fe deficiency treatment (Supplemental Fig. S1A). To confirm the result, anti-MdSIZ1-specific antibodies were custom made (Supplemental Fig. S1B) and used for detection of MdSIZ1 protein levels by western blot assays. The result showed that the protein abundance of MdSIZ1 increased with Fe deficiency in 'Gala' apple plants (Supplemental Fig. S1, C and D). Together, these observations suggest that MdSIZ1 functions as an important protein in response to Fe deficiency in apples.

In soil, for each unit increase in pH, Fe solubility decreases up to 1,000-fold (Santi and Schmidt, 2009). To examine whether MdSIZ1 regulates PM $H^+$-ATPase-mediated rhizosphere acidification and Fe homeostasis in apples, an *MdSIZ1* RNAi vector containing a 35S:DsRED1 cassette was constructed and transiently transformed into the root cells of 'Gala' apple via *Agrobacterium rhizogenes*-mediated genetic transformation, while an empty vector was used as a control. The *MdSIZ1* transcripts were remarkably downregulated in the roots of these plants (Supplemental Fig. S2),

indicating that chimeric plants composed of transgenic roots and wild-type shoots were successfully obtained. Two batches of chimeric transgenic plants denoted as #1 and #2 were used to detect Fe acquisition and PM $H^+$-ATPase $H^+$-transport activity. The results showed that chimeric plants with transgenic *MdSIZ1*-RNAi roots exhibited more serious leaf chlorosis in pH 8.0 alkaline medium than those with the control roots, while none of the plants showed leaf chlorosis in pH 6.0 normal medium (Fig. 1A).

Furthermore, Fe contents were measured in the shoots and roots, respectively. It was found that chimeric transgenic plants grown in pH 8.0 medium, but not in pH 6.0 medium, accumulated 52% less Fe in their shoots and 59% less in their roots compared with empty vector controls (Fig. 1, B and C). Subsequently, PM $H^+$-ATPase $H^+$-transport activity was assessed. The results showed that transgenic *MdSIZ1*-RNAi roots grown in pH 8.0 medium exhibited lower PM $H^+$-ATPase $H^+$-transport activity than the empty vector controls (Fig. 1D). Finally, it was found that transgenic *MdSIZ1*-RNAi roots grown in pH 8.0 medium released less $H^+$ than the empty vector controls, as indicated by the yellow color around the roots after staining with bromocresol purple (Fig. 1E).

As it is difficult to obtain transgenic apple plants overexpressing *MdSIZ1*, *MdSIZ1* was ectopically expressed in Arabidopsis to further characterize if MdSIZ1 functions in the regulation of the PM $H^+$-ATPase-mediated response to Fe acquisition in planta. Three independent transgenic lines, OE13, OE19, and OE33, were chosen for further analysis (Fig. 2A). When allowed to grow in pH 6.0 medium, transgenic seedlings exhibited longer roots than the wild-type controls, but no other phenotype was observed. When grown in pH 8.0 medium, transgenic seedlings exhibited a higher tolerance to Fe deficiency, as indicated by more growth, than the wild-type controls. Moreover, in pH 8.0 medium, these transgenic seedlings produced more chlorophyll, accumulated more Fe, exhibited greater PM $H^+$-ATPase $H^+$-transport activity, and released more $H^+$ into the medium than the wild-type controls (Fig. 2, B–G).

In addition, the results from assessment of apple calli showed that the overexpression of *MdSIZ1* resulted in higher PM $H^+$-ATPase $H^+$-transport activity compared with wild type and the controls, while *MdSIZ1* suppression lowered this activity, leading to a similar trend in Fe acquisition under alkaline conditions as observed in the transgenic Arabidopsis plants (Supplemental Fig. S3). Taken together, these results indicated that MdSIZ1 plays an important role in the regulation of PM $H^+$-ATPase-mediated acidification capacity and Fe acquisition in plants.

### MdSIZ1 Interacts with MdbHLH104 Both In Vitro and In Vivo

To investigate how MdSIZ1 regulates PM $H^+$-ATPase-mediated acidification capacity and Fe acquisition, a yeast two-hybrid (Y2H) screen was performed to identify MdSIZ1-interacting proteins. As a result, several positive colonies were obtained. One of them contained a partial cDNA fragment of the *MdbHLH104* gene, which was previously reported to be a positive regulator of PM $H^+$-ATPase activity in apple plants (Supplemental Fig. S4A; Zhao et al., 2016a).

Y2H assays were conducted to confirm that MdSIZ1 interacts with the full length MdbHLH104 protein. MdSCE1 (SUMO E2 Conjugating Enzyme 1), which is a homolog of AtSCE1, and a pGAD empty vector were used as positive and negative controls, respectively. Yeast cells coexpressing AD-MdbHLH104+BD-MdSIZ1 or AD-MdSCE1+BD-MdSIZ1, but not those coexpressing pGAD+BD-MdSIZ1, grew on SD/-Trp/-Leu/-His/-Ade screening medium (Fig. 3A), indicating that MdSIZ1 interacted with MdbHLH104 in yeast cells.

Importantly, MdSIZ1 did not interact with other IVc subgroup bHLH TFs, such as MdbHLH105, MdbHLH115, MdbHLH11, MdbHLH121, or MdPYE, which are reported to be involved in the regulation of Fe homeostasis (Supplemental Fig. S4B; Zhao et al., 2016a). Therefore, MdSIZ1 specifically interacted with MdbHLH104 in yeast cells.

The physical interaction between MdSIZ1 and MdbHLH104 was further confirmed using an in vitro pull-down assay. The results showed that His-MdSIZ1 and GST-MdbHLH104 were both detected in whole-cell lysates (Input). MdSIZ1 was not detected in the control sample (GST protein alone), whereas MdSIZ1 fused with a His tag was pulled down via GST-MdbHLH104 (Fig. 3B), indicating that MdSIZ1 directly interacted with MdbHLH104.

To further confirm their interaction in vivo, a coimmunoprecipitation (Co-IP) assay was performed. Total proteins extracted from *35S:MdbHLH104-GFP* (*MdbHLH104-GFP*) and *35S:GFP* (pBIN) transgenic apple plants (Zhao et al., 2016a) were used to carry out the immunoprecipitation using anti-GFP antibodies. As a result, MdSIZ1 was detected in the pellet fraction (IP) of *MdbHLH104-GFP* transgenic plants but not in that of the pBIN control (Fig. 3C), indicating that MdSIZ1 interacted with MdbHLH104 in vivo.

Bimolecular fluorescence complementation (BiFC) assays were also employed to examine the MdSIZ1-MdbHLH104 interaction *in planta*. The *MdbHLH104* gene sequence fused in frame with the 5′ end of a gene sequence encoding the C-terminal half of yellow fluorescent protein (MdbHLH104-cYFP) and the MdSIZ1 gene sequence fused in frame with the 3′ end of a gene sequence encoding the N-terminal half of YFP (MdSIZ1-nYFP) were transiently coexpressed in tobacco leaves. It was found that MdSIZ1 interacted with MdbHLH104 in the nucleus (Fig. 3D), indicating that MdSIZ1 and MdbHLH104 colocalize inside the cell.

Taken together, these observations indicate that MdSIZ1 interacts with MdbHLH104 both in vitro and in vivo.

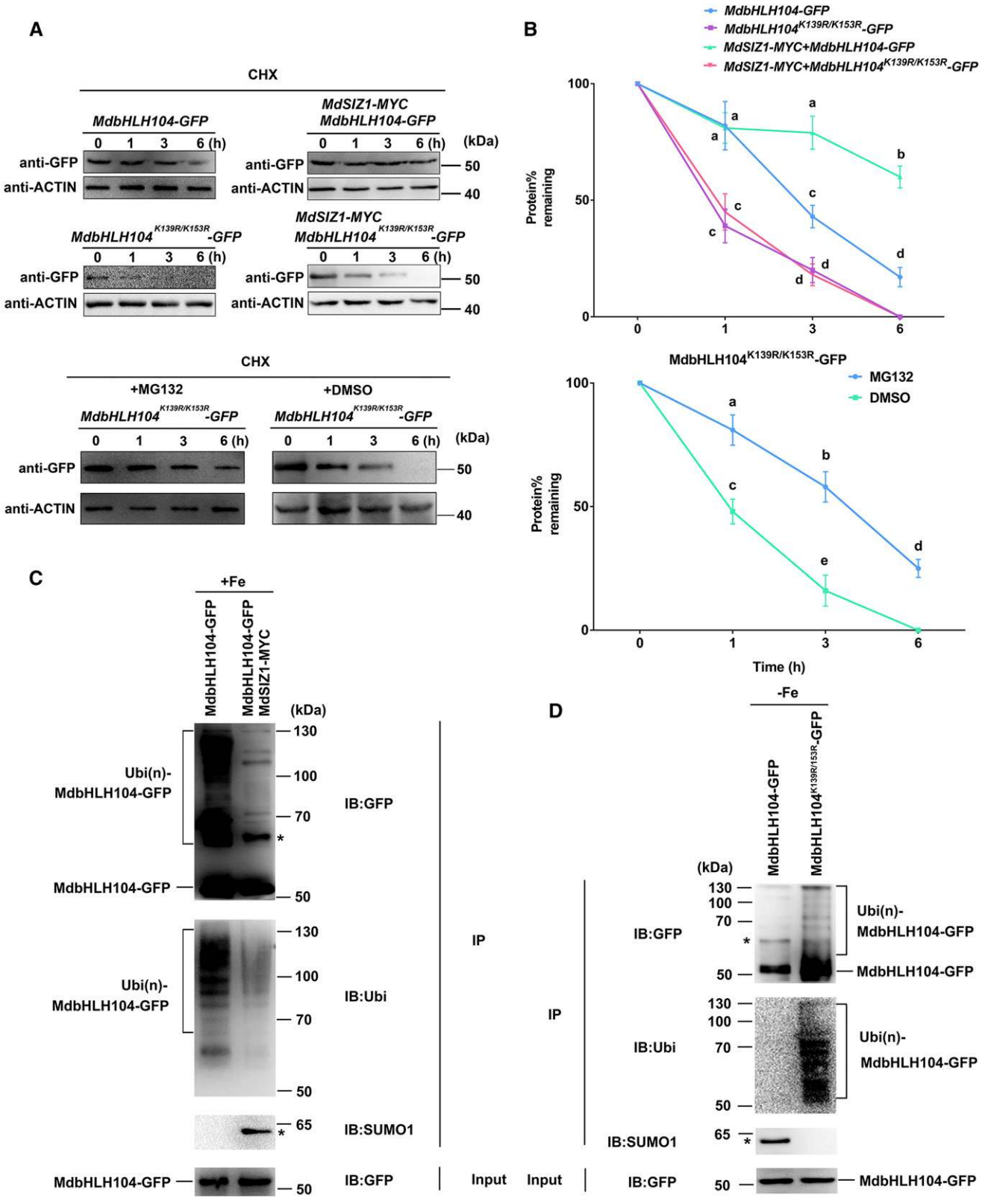


**Figure 5.** MdSIZ1 stabilizes MdbHLH104 and inhibits its ubiquitination. A, MdbHLH104 protein degradation assay in vivo. After pretreatment in Fe-deficient conditions for 1 h, four transgenic calli, *MdbHLH104-GFP*, *MdbHLH104-GFP/MdSIZ1-MYC*, *MdbHLH104*$^{K139R/K153R}$*-GFP*, and *MdbHLH104*$^{K139R/K153R}$*-GFP/MdSIZ1-MYC* were placed in the Fe-sufficient fluid medium containing 250 μM translational inhibitor cycloheximide (CHX) for different durations and sampled simultaneously to detect

### MdSIZ1 directly sumoylates MdbHLH104 proteins at residues K139 and K153 under conditions of Fe deficiency

Considering MdSIZ1 functions as a SUMO E3 ligase (Zhou et al., 2017) and that it interacts with MdbHLH104, it is reasonable to hypothesize that MdSIZ1 may directly sumoylate the MdbHLH104 protein. Subsequently, the putative sumoylation site consensus sequence $\varphi$-K-X-E/D ($\varphi$ represents a hydrophobic amino acid, K represents the Lys that is conjugated to SUMO, X represents any amino acid, and E/D represents an acidic residue) (Sampson et al., 2001) was identified in MdbHLH104 using SUMOplot (http://www.abgent.com/sumoplot) analysis (Lin et al., 2016). It was found that two sumoylation sites with high conservation among different plant species exist in MdbHLH104 (LK139AE and LK153AD), suggesting that it may be a SUMO substrate (Supplemental Fig. S5). To test whether MdbHLH104 is a substrate of MdSIZ1, an in vitro sumoylation assay was performed. Recombinant GST-MdbHLH104 was incubated with SUMO-activating enzyme E1, SUMO-conjugating enzyme E2, SUMO1, and recombinant His-MdSIZ1, followed by immunoblot analysis. The results showed that SUMO1-MdbHLH104 conjugates were not detected by either anti-GST or anti-SUMO1 antibodies in the absence of MdSIZ1, but conjugates were detected when all components were present (Fig. 4A), indicating that MdSIZ1 directly sumoylated MdbHLH104 in vitro. In addition, the single substitution of K-to-R of either the K139 or K153 site did not block the MdbHLH104-SUMO1 conjugation; however, double substitution at both sites did block conjugation, indicating that both K139 and K153 were crucial sites for SUMO conjugation of MdbHLH104.

To examine whether Fe deficiency could induce sumoylation of MdbHLH104 proteins, *MdbHLH104-GFP* transgenic plants of line L1 were used (Zhao et al., 2016a). MdbHLH104-GFP proteins extracted from transgenic plants treated with or without Fe deficiency were immunoprecipitated with an anti-GFP antibody and then subjected to western blot analysis with anti-GFP and anti-SUMO1 antibodies, respectively. The result showed that the MdbHLH104 protein exhibited higher sumoylation levels under Fe-deficient conditions than under Fe-sufficient conditions (Fig. 4B), indicating that Fe deficiency could induce SUMO modification of MdbHLH104 proteins in apple plants.

To examine whether amino acids K139 and K153 were crucial for Fe-induced sumoylation of MdbHLH104 in vivo, transgenic apple calli *MdbHLH104-GFP* and *MdbHLH104*$^{K139R/K153R}$*-GFP* were obtained and used for sumoylation detection (Supplemental Fig. S6, B and C). The result showed that Fe deficiency induced SUMO modification of MdbHLH104 proteins in apple calli, similar to that observed in transgenic plants, and that double mutation of K139R/K153R in the MdbHLH104 protein abolished this sumoylation (Fig. 4C), indicating that K139 and K153 were crucial for Fe deficiency-induced sumoylation of MdbHLH104. In addition, double transgenic calli *MdbHLH104-GFP/MdSIZ1-MYC* and *MdbHLH104-GFP/antiMdSIZ1* were obtained (Supplemental Fig. S6, B and C). It was found that *MdSIZ1* overexpression enhanced the sumoylation levels of the MdbHLH104 protein in response to Fe deficiency, while its suppression remarkably decreased the sumoylation levels (Fig. 4C), suggesting that MdSIZ1 was involved in Fe deficiency-induced sumoylation of the MdbHLH104 protein.

### MdSIZ1 stabilizes MdbHLH104 and inhibits its ubiquitination

To further investigate how MdSIZ1 influences MdbHLH104, protein degradation assays were performed. After pretreatment in Fe-deficient conditions for 1 h, four types of transgenic calli, *MdbHLH104-GFP*, *MdbHLH104-GFP/MdSIZ1-MYC*, *MdbHLH104*$^{K139R/K153R}$*-GFP*, and *MdbHLH104*$^{K139R/K153R}$*-GFP/MdSIZ1-MYC*, were treated under Fe-sufficient conditions for different durations. The results showed that the substitution of K-to-R of residues K139 and K153 clearly increased the degradation rate of the MdbHLH104-GFP proteins (Fig. 5, A and B). In addition, *MdSIZ1* overexpression inhibited the proteolysis of MdbHLH104-GFP, but not MdbHLH104$^{K139R/K153R}$-GFP, indicating that MdSIZ1-mediated sumoylation of the MdbHLH104-GFP protein promoted its abundance.

To exclude the possibility that the observed change in MdbHLH104 protein levels was a result of variation in

**Figure 5.** (*Continued.*)
MdbHLH104-GFP protein abundance using an anti-GFP antibody. For MG132 (26S proteasome inhibitor) treatment, the Fe deficiency pretreated transgenic calli were treated with 50 μM MG132 for 6 h and then used for protein degradation assay. ACTIN in total protein extracts was used as a loading control. DMSO was used as a negative control for MG132. B, Quantification of MdbHLH104-GFP protein levels using Quantity One software (Bio-Rad). The protein degradation assay in A was carried out three times, and the protein quantities relative to the levels at initial time 0 were counted and used to calculate the SD, as indicated by the error bars. Samples denoted by different letters are significantly different ($P < 0.01$, ANOVA, Tukey correction). C and D, Ubiquitination of MdbHLH104-GFP proteins in *MdbHLH104-GFP*, *MdbHLH104-GFP/MdSIZ1-MYC*, and *MdbHLH104*$^{K139R/K153R}$*-GFP* transgenic calli under Fe-sufficient or Fe-deficient conditions. The Fe-deficient pretreated transgenic calli were treated with 50 μM MG132 for 6 h and then treated in Fe-sufficient conditions for 6 h or not. Then, MdbHLH104-GFP proteins were IPed using an anti-GFP antibody. MdbHLH104-GFP proteins in whole-cell lysates prior to treatment (Input) and in the pellet fraction (IP) or ubiquitinated MdbHLH104 proteins in the pellet fraction (IP) were detected via immunoblot analysis with anti-GFP and antiubiquitin antibodies, respectively. The sumoylated MdbHLH104 proteins in the pellet fraction (IP) were detected by anti-SUMO1 antibodies. Asterisks indicate sumoylated MdbHLH104 bands. IB, Immunoblot.

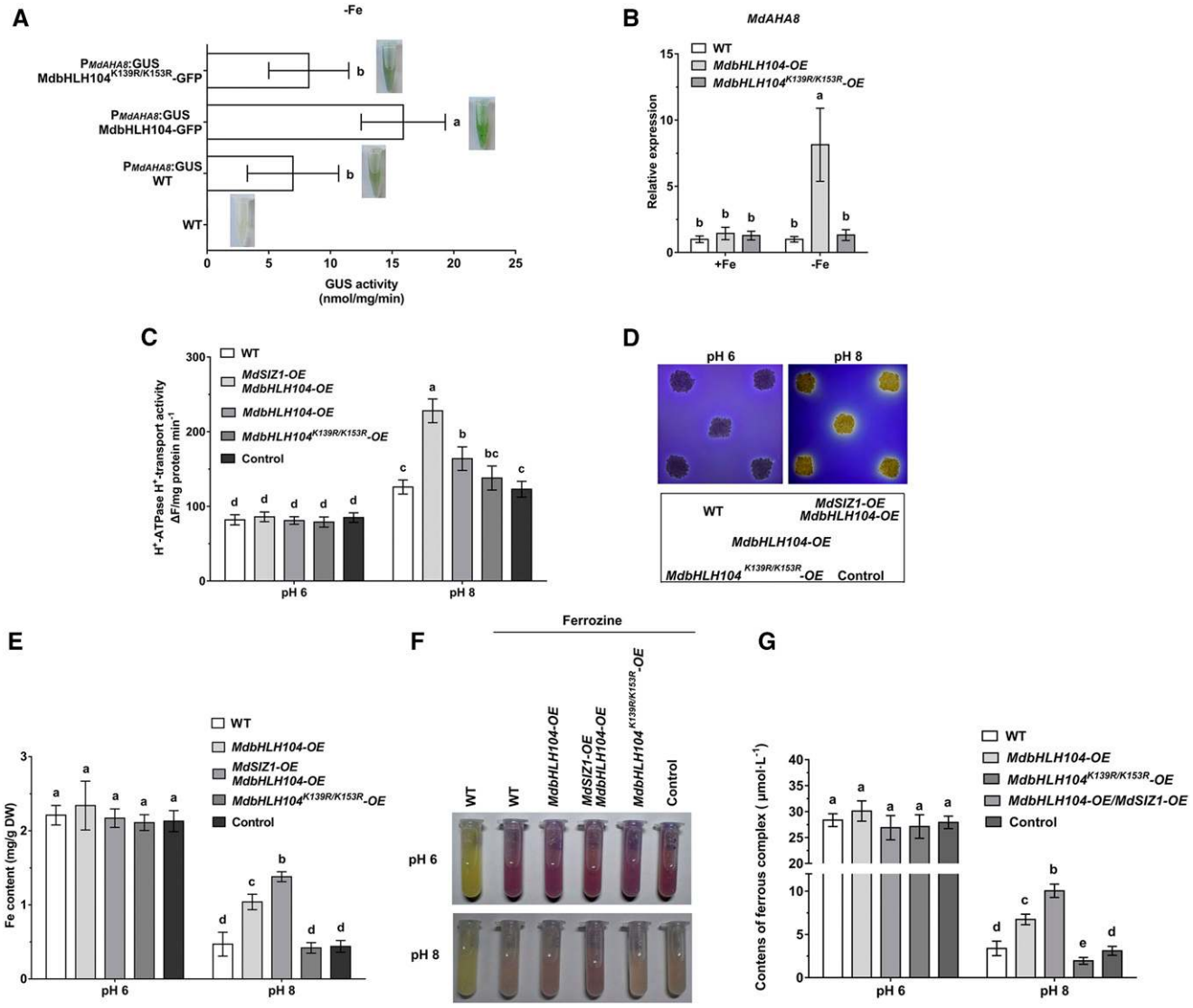


**Figure 6.** MdbHLH104 sumoylation at residues K139 and K153 is crucial for its function in activating *MdAHA8* transcription and promoting Fe acquisition. A, Promoter activity assays using GUS staining and GUS activity assays. The 2-week-old transgenic calli were treated in Fe-deficient conditions for 5 d and then used for GUS staining and GUS activity measurements. B, *MdAHA8* expression as measured by RT-qPCR in wild type, *MdbHLH104-OE*, and *MdbHLH104*$^{K139R/K153R}$*-OE* transgenic calli under Fe-sufficient or -deficient conditions, respectively. C, PM $H^+$-ATPase $H^+$-transport activity of wild type, *MdbHLH104-OE/MdSIZ1-OE*, *MdbHLH104-OE*, *MdbHLH104*$^{K139R/K153R}$*-OE*, and control (*35S:GFP*) transgenic apple calli. The 2-week-old transgenic calli were grown on pH 6 or pH 8 media for 5 d and then used for PM $H^+$-ATPase $H^+$-transport activity detection. D, Acidification of transgenic apple calli. The 2-week-old transgenic calli were grown on pH 6 or pH 8 media for 5 d and then transferred to bromocresol purple medium for 36 h. Acidification is indicated as a yellow color around the apple calli. E, Fe content of wild-type, *MdbHLH104-OE/MdSIZ1-OE*, *MdbHLH104-OE*, *MdbHLH104*$^{K139R/K153R}$*-OE*, and control (*35S:GFP*) transgenic apple calli. The 2-week-old transgenic calli were grown on pH 6 or pH 8 media for 5 d and then used for Fe content measurement. DW, dry weight. F, Visualization of ferrous iron in wild type, *MdbHLH104-OE/MdSIZ1-OE*, *MdbHLH104-OE*, *MdbHLH104*$^{K139R/K153R}$*-OE*, and control (*35S:GFP*) transgenic apple calli. Ferrous iron is indicated by red-colored complex formed by the Ferrozine reagent. G, Quantified measurements of ferrous complex of ferrozine in F. The optical density (OD) of the complex was measured at 562 nm wavelength, and the concentration of the complex was calculated according to Lambert-Beer law. Error bars indicate the SD for three biological replicates in which the experiments were carried out three times using the calli of each line. Samples denoted by different letters are significantly different ($P < 0.01$, ANOVA, Tukey correction).

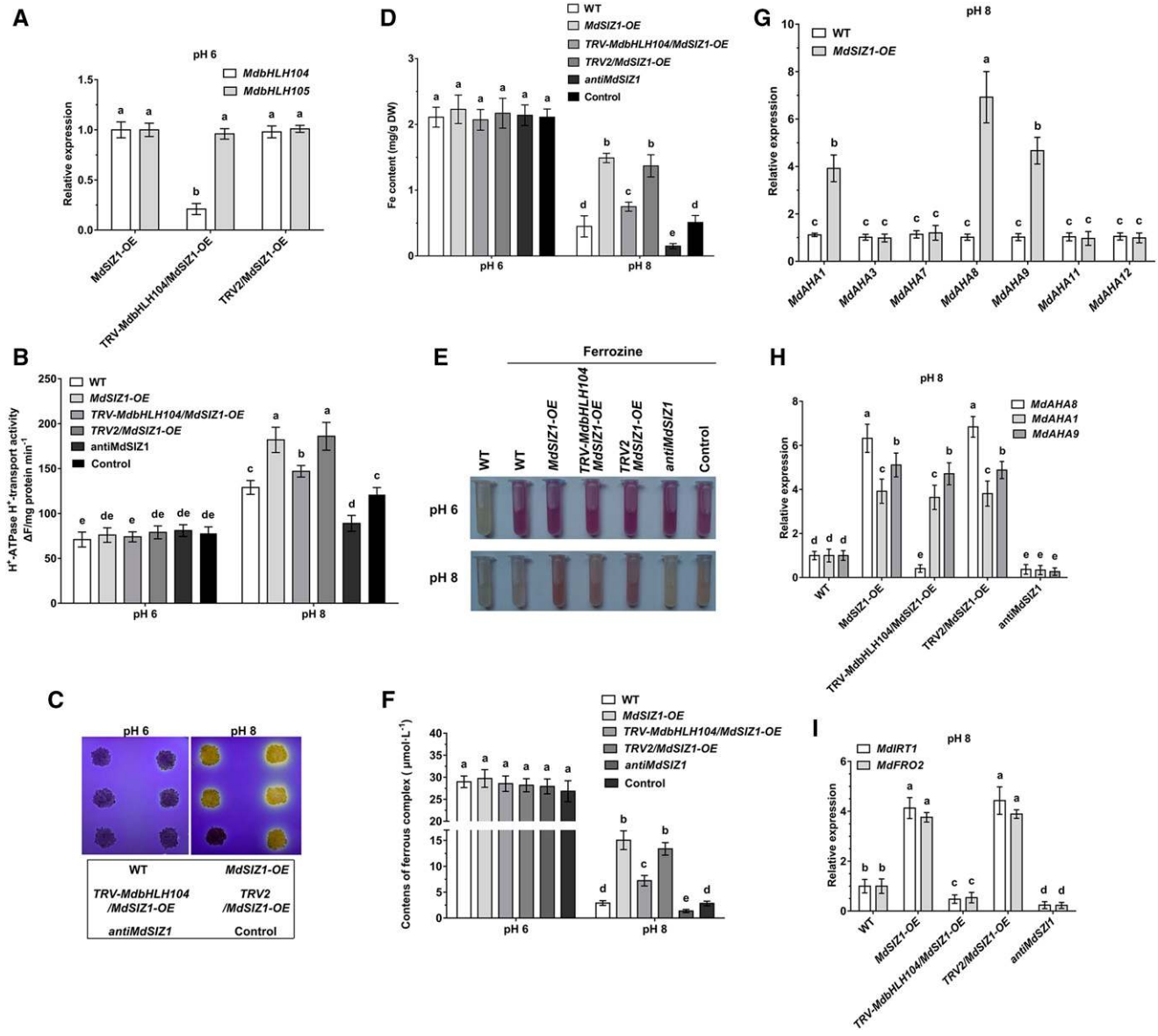


**Figure 7.** Transient silencing of *MdbHLH104* in the background of *MdSIZ1-OE* partially inhibited its function in promoting PM $H^+$-ATPase-mediated acidification capacity and Fe homeostasis. A, Silencing of *MdbHLH104* by the *TRV-MdbHLH104* vector in the background of *MdSIZ1-OE* transgenic calli. The *MdbHLH104* fragment was amplified and cloned into the tobacco rattle virus (TRV) vector to transiently silence the expression of *MdbHLH104* in the background of *MdSIZ1-OE* transgenic calli. The expression of *MdbHLH105* was used as a negative control. B, PM $H^+$-ATPase $H^+$-transport activity of wild type (WT), *MdSIZ1-OE*, *TRV-MdbHLH104/MdSIZ1-OE*, *TRV2/MdSIZ1-OE*, *antiMdSIZ1*, and control (*35S:MYC*) transgenic apple calli. The 2-week-old transgenic calli and the calli that had been treated with TRV were grown on pH 6 or pH 8 media for 5 d and then used for PM $H^+$-ATPase $H^+$-transport activity detection. C, Acidification of transgenic apple calli. The 2-week-old transgenic calli and the calli that had been treated by TRV were grown on pH 6 or pH 8 media for 5 d and then transferred to bromocresol purple medium for 36 h. Acidification is indicated by the yellow color around the apple calli. D, Fe contents of wild type, *MdSIZ1-OE*, *TRV-MdbHLH104/MdSIZ1-OE*, *TRV2/MdSIZ1-OE*, *antiMdSIZ1*, and control (*35S:MYC*) transgenic apple calli. The 2-week-old transgenic calli and the calli that had been treated with TRV were grown on pH 6 or pH 8 media for 5 d and then used for Fe content measurement. DW, dry weight. E, Visualization of ferrous iron in wild type, *MdSIZ1-OE*, *TRV-MdbHLH104/MdSIZ1-OE*, *TRV2/MdSIZ1-OE*, *antiMdSIZ1*, and control (*35S:MYC*) transgenic apple calli. Ferrous iron is indicated by the red-colored complex formed by Ferrozine reagent. F, Quantified measurements of ferrous complex of ferrozine in E. The OD of the complex was measured at 562-nm wavelength, and the concentration of the complex was calculated according to Lambert-Beer law. G, The expression of *MdAHA1*, *MdAHA3*, *MdAHA7*, *MdAHA8*, *MdAHA9*, *MdAHA11*, and *MdAHA12*, as measured by RT-qPCR, in wild type and *MdSIZ1-OE* transgenic calli at pH 8. The 2-week-old wild-type and *MdSIZ1-OE* transgenic calli were treated with pH 8 media and then used for gene expression detection. H, *MdAHA1*, *MdAHA8*, and *MdAHA9* expression in wild type, *MdSIZ1-OE*, *TRV-MdbHLH104/MdSIZ1-OE*, *TRV2/MdSIZ1-OE*, and *antiMdSIZ1* transgenic

transcription levels, an RT-qPCR assay was performed using *MdSIZ1*-overexpression and *MdSIZ1*-suppression transgenic calli. The data indicated that there was no difference in the transcript levels of *MdbHLH104* in wild type, *MdSIZ1-OE*, or *antiMdSIZ1* transgenic calli in both Fe-sufficient and Fe-deficient conditions (Supplemental Fig. S7), suggesting that MdSIZ1 affected MdbHLH104 abundance at the protein level. Taken together, these results indicated that MdSIZ1-mediated sumoylation at residues K139 and K153 of MdbHLH104 promotes its stability.

In addition, treatment with the 26S proteasome inhibitor MG132 noticeably inhibited the degradation of the MdbHLH104 proteins caused by the mutation of sumoylation sites (Fig. 5, A and B), indicating that MdSIZ1 may stabilize the MdbHLH104 protein by inhibiting its proteolysis via the 26S proteasome, which is generally associated with ubiquitin modifications. To determine whether MdSIZ1-mediated sumoylation influences MdbHLH104 protein ubiquitination, MdbHLH104 proteins were immunoprecipitated with anti-GFP antibodies from three types of transgenic calli, *MdbHLH104-GFP*, *MdbHLH104-GFP/MdSIZ1-MYC*, and *MdbHLH104$^{K139R/K153R}$-GFP*, followed by western blot analysis. The result indicated that the *MdbHLH104-GFP* transgenic calli generated more high-molecular-mass forms of MdbHLH104-GFP under Fe-sufficient conditions than under Fe-deficient conditions (Fig. 5, C and D). However, overexpression of *MdSIZ1* in the *MdbHLH104-GFP* background inhibited this ubiquitination (Fig. 5C). In contrast, mutation of the sumoylation sites in MdbHLH104-GFP clearly promoted its ubiquitin modification under conditions of Fe deficiency (Fig. 5D). Thus, MdSIZ1-mediated sumoylation of MdbHLH104 inhibited its ubiquitination.

### MdbHLH104 Sumoylation at Residues K139 and K153 Is Crucial for Its Function in Activating *MdAHA8* Transcription and Promoting Fe Acquisition

To examine whether the sumoylation of MdbHLH104 was required for its function in activating the transcription of *MdAHA8*, a *pMdAHA8:GUS* construct was genetically transformed into apple calli. Subsequently, the constructs *MdbHLH104-GFP* and *MdbHLH104$^{K139R/K153R}$-GFP* were introduced into *pMdAHA8:GUS* transgenic calli (Supplemental Fig. S6A). As a result, *pMdAHA8:GUS/MdbHLH104-GFP* double-transgenic calli showed higher GUS activity than the *pMdAHA8:GUS* alone. However, mutation of the sumoylation sites in MdbHLH104 remarkably decreased the activation of the *MdAHA8* promoter (Fig. 6A). Moreover, RT-qPCR assays showed that the expression levels of *MdAHA8* were noticeably induced in *MdbHLH104-GFP* but not in *MdbHLH104$^{K139R/K153R}$-GFP* transgenic calli under the conditions of Fe deficiency (Fig. 6B). Taken together, these results indicated that the sumoylation of MdbHLH104 is required for its function in activating the transcription of *MdAHA8*.

Subsequently, wild-type and four transgenic calli, 35S:MdbHLH104-GFP (MdbHLH104-OE), 35S:MdbHLH104-GFP/35S:MdSIZ1-MYC (MdbHLH104-OE/MdSIZ1-OE), 35S:MdbHLH104$^{K139R/K153R}$-GFP (MdbHLH104$^{K139R/K153R}$-OE), and 35S:GFP (control), were used to assess PM H$^+$-ATPase-mediated acidification capacity and Fe acquisition. Under normal (pH 6) conditions, there was no significant difference among the five calli. When cultivated under alkaline (pH 8) conditions, however, MdbHLH104-OE exhibited higher PM H$^+$-ATPase H$^+$-transport activity than the wild type and control. Furthermore, it was found that the promotion of PM H$^+$-ATPase H$^+$-transport activity was reduced when the sumoylation sites of MdbHLH104 were mutated (Fig. 6, C and D). Furthermore, when MdSIZ1 was overexpressed in MdbHLH104 transgenic calli, the double transgenic calli MdbHLH104-OE/MdSIZ1-OE exhibited the highest PM H$^+$-ATPase H$^+$-transport activity (Fig. 6, C and D), as determined by Fe content and $Fe^{2+}$ staining with Ferrozine (Fig. 6, E–G). Taken together, these results indicated that MdbHLH104 sumoylation at residue K139 and K153 was crucial for its function in promoting PM H$^+$-ATPase-mediated acidification capacity and Fe acquisition.

### MdSIZ1 Promoted PM H$^+$-ATPase-Mediated Acidification Capacity and Fe Homeostasis Is Partially MdbHLH104 Dependent

To further examine whether the MdSIZ1-mediated increase in PM H$^+$-ATPase-mediated acidification capacity was dependent on MdbHLH104, the viral vector *TRV-MdbHLH104* was transiently transformed into *MdSIZ1-OE* transgenic calli. The empty vector *TRV2* was used as a negative control. As a result, the expression of *MdbHLH104*, but not *MdbHLH105*, was specifically inhibited in the *TRV-MdbHLH104/MdSIZ1-OE* transgenic calli (Fig. 7A).

Subsequently, wild-type and four transgenic calli, *MdSIZ1-OE* (*35S:MdSIZ1-MYC*), *TRV-MdbHLH104/MdSIZ1-OE*, *TRV2/MdSIZ1-OE*, *antiMdSIZ1* (*35S:antiMdSIZ1*), and an empty vector *35S:MYC* control were

**Figure 7.** (*Continued*.)
apple calli under pH 8. The 2-week-old transgenic calli and the calli that had been treated by TRV were grown at pH 8 for 5 d and then used for gene expression detection. I, *MdFRO2* and *MdIRT1* expression in wild type, *MdSIZ1-OE*, *TRV-MdbHLH104/MdSIZ1-OE*, *TRV2/MdSIZ1-OE*, and *antiMdSIZ1* apple calli at pH 8. The 2-week-old transgenic calli and the calli that had been treated with TRV were treated with pH 8 media for 5 d and then used for gene expression detection. Error bars indicate the SD for three biological replicates in which the experiments were carried out three times using the calli of each line. Samples denoted by different letters are significantly different ($P < 0.01$, ANOVA, Tukey correction).

used for further investigation of PM $H^+$-ATPase-mediated acidification capacity and Fe acquisition. The results showed that, under alkaline conditions, *MdSIZ1* overexpression remarkably enhanced PM $H^+$-ATPase $H^+$-transport activity and Fe content in transgenic calli, while its suppression decreased PM $H^+$-ATPase $H^+$-transport activity and Fe content (Fig. 7, B–F). Moreover, it was found that *MdbHLH104* suppression partially abolished MdSIZ1-mediated promotion of PM $H^+$-ATPase-mediated acidification capacity and Fe acquisition in *TRV-MdbHLH104/MdSIZ1-OE* transgenic calli (Fig. 7, B–F). These results indicated that other MdAHAs may also be regulated by MdSIZ1, and MdSIZ1 promotion of PM $H^+$-ATPase-mediated acidification capacity and Fe homeostasis was at least partially dependent on MdbHLH104.

In apple plants, seven MdAHAs are possibly responsible for rhizosphere acidification, and MdAHA8 is directly regulated by MdbHLH104 (Zhao et al., 2016a). None of these MdAHAs interacted with MdSIZ1 (Supplemental Fig. S8). RT-qPCR assays demonstrated that MdSIZ1 positively modulated the transcript levels of three *MdAHA* genes (*MdAHA1*, *MdAHA8*, and *MdAHA9*) (Fig. 7G). Moreover, it was found that *MdbHLH104* suppression completely abolished the MdSIZ1-mediated increase in *MdAHA8* transcripts, but not that of *MdAHA1* and *MdAHA9*. In contrast, *MdSIZ1* suppression inhibited the expression of all three genes in the *antiMdSIZ1* transgenic calli (Fig. 7H), indicating that MdSIZ1 directly regulated the expression of *MdAHA8* in an MdbHLH104-dependent manner, but it indirectly modulated the transcription of *MdAHA1* and *MdAHA9* in an MdbHLH104-independent manner.

The ferric reduction assays in Figures 6F and 7E indicated that MdSIZ1 may be involved in the regulation of responses downstream of ferric reduction, such as those mediated by FIT and the Ib subgroup bHLH TFs. In apple, it was found that MdbHLH104 directly binds to the promoters of two Ib subgroup bHLH genes, *MdbHLH38* and *MdbHLH39* (Zhao et al., 2016a). We thus detected the transcript levels of *MdbHLH38* and *MdbHLH39* in the wild type, *MdbHLH104-OE*, *MdSIZ1-OE*, and *antiMdSIZ1* transgenic calli by RT-qPCR assays. The results showed that MdbHLH104 and MdSIZ1 positively regulated *MdbHLH38* and *MdbHLH39* expression in pH 8 conditions (Supplemental Fig. S9), indicating that sumoylation of MdbHLH104 mediated by MdSIZ1 promoted the ferric reduction processes in apple in part through MdbHLH38 and MdbHLH39.

Subsequently, the transcript levels of *MdFRO2* and *MdIRT1*, which play crucial roles in $Fe^{3+}$ reduction and $Fe^{2+}$ absorption, were detected by RT-qPCR assays. It was found that *MdbHLH104* suppression partially abolished the MdSIZ1-mediated increase in *MdFRO2* and *MdIRT1* transcripts. In contrast, *MdSIZ1* suppression inhibited the expression of all genes tested in the *antiMdSIZ1* transgenic calli (Fig. 7I). These results suggested that MdSIZ1 regulated the expression of *MdFRO2* and *MdIRT1*, partially dependent on MdbHLH104. Taken together, these observations indicated that MdSIZ1 promoted PM $H^+$-ATPase-mediated acidification capacity and Fe homeostasis by partially depending on MdbHLH104.

## DISCUSSION

Plants undergo various abiotic stresses during growth and development. Among the E3 ligase enzymes involved in sumoylation, SIZ1 participates in the regulation of processes related to various abiotic stresses, such as phosphate starvation, low temperature, drought, and ABA, via direct modification of target proteins (Miura et al., 2005, 2007; Catala et al., 2007; Zheng et al., 2012; Zhou et al., 2017). In addition, the bHLH TF MdbHLH104 directly regulates the *MdAHA8* gene to modulate PM $H^+$-ATPase-mediated rhizosphere acidification and Fe homeostasis (Zhao et al., 2016a). Here, it was found that the apple SUMO E3 ligase MdSIZ1 interacted with and sumoylated MdbHLH104, thereby promoting PM $H^+$-ATPase-mediated rhizosphere acidification and regulating Fe homeostasis.

In most cases, SIZ1-mediated sumoylation of target proteins occurs at only one site, which contains the consensus sequence $\varphi$-K-X-E/D (Sampson et al., 2001). For example, Arabidopsis SIZ1 sumoylates the MYB30, ICE1, and COP1 proteins at their K283, K393, and K193 residues, respectively (Miura et al., 2007; Zheng et al., 2012; Lin et al., 2016). In this study, however, it was found that MdSIZ1 sumoylated MdbHLH104 at two residues, K139 and K153 (Fig. 4). These two sumoylation sites are highly conserved among bHLH104 homologs in both dicotyledonous and graminaceous plants (Supplemental Fig. S4), suggesting a novel sumoylation pattern for MdbHLH104 in plants.

According to previous studies, in contrast to ubiquitination, in which the substrate proteins were recognized by and interacted with various E3 ligases, a single E2 recognizes the sumoylation site consensus sequence $\varphi$-K-X-E/D and E3 recognizes additional target proteins in sumoylation (Sampson et al., 2001; Flotho and Melchior, 2013). During the sumoylation process, the E3 ligase enzyme binds to the E2 conjugating enzyme and promotes the transfer of SUMO to the target proteins (Gill, 2004). In this study, a bHLH TF, MdbHLH104, was identified as a direct target protein of SUMO E3 ligase MdSIZ1, and mutation of sumoylation sites inhibited the SUMO modification of MdbHLH104 by MdSIZ1. These results suggest that in the process of sumoylation of MdbHLH104, the E3 ligase MdSIZ1 locks the flexible SUMO ~ MdSCE1 thioester bond in an orientation that is favorable for nucleophilic attack by the target Lys.

In plants, the HLH region of bHLH TFs facilitates the formation of homodimers and/or heterodimers, which may play a critical role in the determination of gene function (Leivar et al., 2008). In Arabidopsis, bHLH104 interacts with bHLH105 to modulate Fe homeostasis

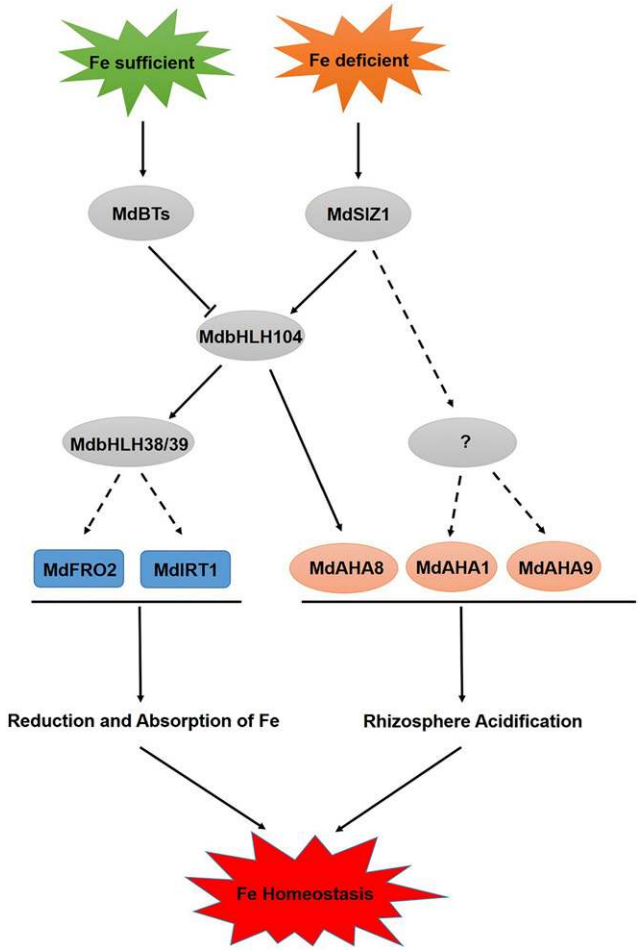


**Figure 8.** A model of MdSIZ1-mediated sumoylation in the regulation the apple plant's response to Fe deficiency. Under Fe-deficient conditions, the sumoylation of MdbHLH104 and other unknown TFs mediated by MdSIZ1 promotes their protein stability. Stabilized TFs then bind to the promoters of PM $H^+$-ATPases genes to promote the extrusion of protons to make Fe(III) more soluble. Meanwhile, MdbHLH104 also binds to the promoters of genes encoding Ib subgroup bHLH TFs, like *MdbHLH38* and *MdbHLH39*, to activate their expression. The sumoylation of MdbHLH104 mediated by MdSIZ1 thus promotes the expression of genes downstream of MdbHLH38 and MdbHLH39, such as *MdFRO2* and *MdIRT1*, which converts $Fe^{3+}$ to $Fe^{2+}$ and imports $Fe^{2+}$ across the root epidermal cell membrane to improve tolerance toward Fe deficiency in apple plants. Under Fe-sufficient conditions, E3 ubiquitin ligase and MdBTs (i.e. MdBT1 and MdBT2) target MdbHLH104 and negatively regulate Fe absorption.

(Zhang et al., 2015). The proteins bHLH104, bHLH34, and bHLH105 form heterodimers or homodimers to up-regulate the expression of *bHLH38/39/100/101* and *PYE*, thereby regulating Fe homeostasis (Li et al., 2016). Most recently, it was reported that apple MdbHLH104 forms heterodimers with other IVc subgroup bHLH TFs to activate the transcription of the PM $H^+$-ATPase gene *MdAHA8* (Zhao et al., 2016a). In this study, it was found that MdSIZ1 specifically interacted with and sumoylated MdbHLH104. Thus, MdbHLH104 may play a key role in the IVc subgroup bHLH complex during the MdSIZ1-mediated regulation of PM $H^+$-ATPase activity and Fe homeostasis. Moreover, in addition to *MdAHA8*, the direct target of MdbHLH104, MdSIZ1 also transcriptionally modulated the expression of *MdAHA1* and *MdAHA9* (Fig. 7G), suggesting that MdSIZ1 likely targets other TFs responsible for the transcriptional activity of these genes.

Based on our data, FIT-dependent ferric reduction was activated by MdSIZ1 and MdbHLH104 under Fe deficiency (Figs. 6F and 7E). These results suggest that the sumoylation of MdbHLH104 by MdSIZ1 could induce Ib subgroup bHLH proteins. In Arabidopsis, bHLH104 and bHLH105 formed a heterodimer to bind directly to the promoters of Ib subgroup bHLH genes such as *bHLH38*, *bHLH39*, *bHLH100*, and *bHLH101* (Zhang et al., 2015). FIT interacts with bHLH38/39/100/101 to activate the expression of *IRT1* and *FRO2* (Li et al., 2016). In apple, there are four Ib subgroup bHLH TF members. Among them, MdbHLH104 directly binds to the promoters of two Ib subgroup bHLH genes, *MdbHLH38* and *MdbHLH39* (Zhao et al., 2016a). RT-qPCR

assays showed that the transcript levels of *MdbHLH38* and *MdbHLH39* were efficiently up-regulated by MdbHLH104 and MdSIZ1 under the conditions of Fe deficiency (Supplemental Fig. S9). The sumoylation of MdbHLH104 could promote the expression of *MdbHLH38* and *MdbHLH39* and thus activate the *MdFRO2* and *MdIRT1* gene.

A previous study showed that only *MdbHLH38* and *MdbHLH39* were regulated by MdbHLH104 (Zhao et al., 2016a). Given that suppression of *MdbHLH104* in the *MdSIZ1-OE* background did not completely abolish the MdSIZ1-mediated increase in *MdFRO2* and *MdIRT1* transcripts (Fig. 7I), we suspect that MdSIZ1 may regulate other Ib subgroup bHLH TFs in an MdbHLH104-independent manner. These results suggest that MdSIZ1 serves a global role in regulating Fe homeostasis in plants.

Sumoylation of target proteins in plants is carried out by three enzymatic steps, similar to the ubiquitination pathway. These steps involve the heterodimeric activating enzyme E1 (SAE1 and SAE2), a single E2-conjugating enzyme called SCE1, and two classes of E3 ligase enzymes, including MMS21 and SIZ1 (Miura et al., 2005; Huang et al., 2009; Ishida et al., 2012; Novatchkova et al., 2012). During the sumoylation process, the E3 ligase enzyme binds to the E2-conjugating enzyme and promotes the transfer of SUMO to the target proteins (Gill, 2004). In apples, both *MdSCE1* and *MdSIZ1* were transcriptionally induced by Fe deficiency, and *MdSIZ1* overexpression did not influence the transcript level of *MdSCE1* (Supplemental Fig. S10). Thus, the E2-conjugating enzyme MdSCE1 became a limiting factor when *MdSIZ1* was overexpressed under conditions of Fe sufficiency. This underlies why MdSIZ1-mediated sumoylation of the MdbHLH104 protein and promotion of PM $H^+$-ATPase-mediated acidification capacity occurs only under Fe-deficiency conditions, but not in response to Fe sufficiency, in both plants and calli (Fig. 2, B–G; Supplemental Fig. S2, C–F).

Heterologous expression of MdSIZ1, an apple SUMO E3 ligase, enhanced PM $H^+$-ATPase-mediated rhizosphere acidification and Fe uptake in Arabidopsis (Fig. 2), suggesting that the SIZ1-bHLH104-AHA regulatory module and pathway are conserved in plants. In addition to Fe deficiency, PM $H^+$-ATPases are involved in the responses to various abiotic stresses in plants. In *Medicago* (*Medicago sativa*), AHA3 protein levels and $H^+$-ATPase activity are positively induced by salt stress (Sibole et al., 2005). In addition, the soybean (*Glycine max*) PM $H^+$-ATPase gene (Gene accession number AF091303) is transcriptionally induced by aluminum (Al) treatment (Shen et al., 2005). Recently, it has also been reported that the Arabidopsis PM $H^+$-ATPases AHA2 and AHA7 play an important role in $H^+$ efflux at the root tip in response to low-phosphorus stress (Yuan et al., 2017). For the mechanism of SIZ1-mediated sumoylation in regulating plants tolerance to abiotic stresses, most studies have focused on the mechanism of its direct regulation of target proteins related to stresses. For example, SIZ1 targets PHR1 proteins for SUMO modification to regulate the phosphate deficiency response (Miura et al., 2005). On the other hand, SIZ1-mediated sumoylation may also affect plant tolerance to abiotic stresses via regulating PM $H^+$-ATPase activity. Therefore, the conserved SIZ1-bHLH104-AHA regulatory module and pathway in plants serve in abiotic stress resistance processes beyond their role in Fe homeostasis in apple.

Fe is a crucial micronutrient in plants. Both Fe overload and deficiency limit plant growth and development and decrease crop yield and quality, often resulting in death of the plants (Briat et al., 2015; de Souza Pinto et al., 2016). Therefore, plants have evolved sophisticated mechanisms to maintain Fe homeostasis (Zhang et al., 2015; Li et al., 2016; Zhao et al., 2016a, 2016b). MdbHLH104 degradation was inhibited by MG132 (Fig. 5, A–C), suggesting that MdbHLH104 degradation likely occurs via a 26S proteasome pathway. In apple plants, the scaffold protein MdBT2 recruits cullin-RING ubiquitin ligase 3 to form the $MdBT2^{MdCUL3}$ complex, which in turn ubiquitinates and degrades MdbHLH104 (Zhao et al., 2016b). In this study, it was found that MdSIZ1 stabilized MdbHLH104 via SUMO modification, indicating that sumoylation and ubiquitination have antagonistic effects on MdbHLH104. $MdBT2^{MdCUL3}$-mediated degradation of the MdbHLH104 protein under Fe-sufficient conditions prevents injury caused by overaccumulation of Fe. On the other hand, under conditions of Fe deficiency, MdbHLH104 sumoylation plays the opposite role and promotes Fe uptake from the soil, indicating that different posttranscriptional modifications of MdbHLH104 play distinct roles in regulating Fe homeostasis. In addition to MdbHLH104, sumoylation and ubiquitination of the MdMYB1 TF have antagonistic effects on anthocyanin accumulation (Li et al., 2012; Zhou et al., 2017). Thus, sumoylation and ubiquitination play an important role in balancing plant responses to ambient environment signals via the modification of specific target proteins.

Both MdBT2 and MdSIZ1 regulate MdbHLH104 (Fig. 8; Zhao et al., 2016b). As downstream targets of MdbHLH104, PM $H^+$-ATPases are not only involved in Fe uptake, but they also provide energy for absorption and transportation of other nutrients into plant cells by generating electrochemical gradients (Haruta and Sussman, 2012). In soybeans, under Al stress conditions, the phosphorylation of PM $H^+$-ATPases and their interaction with 14-3-3 proteins are inhibited, resulting in inhibition of $NO_3^-$ uptake (Yang et al., 2016). In addition, Ni uptake by wheat (*Triticum aestivum*) roots partially requires increased generation of a proton gradient by PM $H^+$-ATPases (Dalir et al., 2017). Furthermore, PM $H^+$-ATPases play an important role in regulating plant growth and development, as well as in the response to various stresses (Shen et al., 2005; Sibole et al., 2005; Kim et al., 2013), and both BT2 and SIZ1 are expressed in response to various environmental and endogenous signals (Miura et al., 2005; Mandadi et al., 2009; Zheng et al., 2012). Therefore, the MdBT2/MdSIZ1-MdbHLH104-MdAHA8 regulatory module and pathway serve in

multiple processes beyond their role in Fe homeostasis in plants.

## CONCLUSION

In summary, our findings provide new insights into the mechanisms by which plants respond via an MdSIZ1-MdbHLH104-PM $H^+$-ATPase pathway to control the Fe supply status (Fig. 8). Fe deficiency induces sumoylation of the Fe homeostasis-associated bHLH TF MdbHLH104 and other unknown TFs by enhancing the transcript levels of the gene encoding the SUMO E3 ligase MdSIZ1. Sumoylation of target proteins promotes their stability by inhibiting conjugation of ubiquitin molecules. Stabilized MdbHLH104 and other TFs directly or indirectly activate the transcription of genes encoding PM $H^+$-ATPases, such as *MdAHA1*, *MdAHA8*, and *MdAHA9*, to promote rhizosphere acidification. Meanwhile, MdSIZ1 also promotes the expression of *MdbHLH38* and *MdbHLH39* and thus activates the transcription of *MdFRO2* and *MdIRT1* to convert $Fe^{3+}$ to $Fe^{2+}$ and import $Fe^{2+}$ across root epidermal cell membranes into the plants.

## MATERIALS AND METHODS

### Plant Materials and Growth Conditions

The calli of 'Orin' apples were subcultured as described by Zhao et al. (2016a). In brief, the calli were grown on Murashige and Skoog (MS) medium with 1.5 mg/L 2,4-D (2,4-dichlorophenoxyacetic acid) and 0.4 mg/L 6-benzylaminopurine at 25°C in the dark. The Fe-sufficient media was the MS media containing 100 μM Fe(II)-EDTA. The Fe-deficient media was the same without Fe(II)-EDTA. For alkaline treatment, MS media at a pH of 8 was used.

The 'Gala' apple tissue cultures were grown on MS subculture medium containing 0.5 mg/L 6-benzylaminopurine, 0.2 mg/L 1-naphthylacetic acid, and 0.1 mg/L gibberellin for *Agrobacterium rhizogenes*-mediated transformation and other analyses. The Fe-sufficient media was the MS media containing 100 μM Fe(II)-EDTA. The Fe deficient media was the same without Fe(II)-EDTA. For apple plants with transgenic hairy roots, sand with the addition of Hoagland solution (Hoagland and Arnon, 1950) of pH 6 or pH 8 was used.

Arabidopsis thaliana (ecotype 'Columbia') was grown on MS medium at 22°C under a long-day photoperiod (16 h light/8 h dark). For alkaline treatment, the MS media at a pH of 8 was used.

### Vector Construction and Genetic Transformation

The *MdbHLH104-GFP* and *PMdAHA8:GUS* vectors were constructed as described by Zhao et al. (2016a). The *MdSIZ1-MYC* and *antiMdSIZ1* vectors were constructed as described by Zhou et al. (2017). *MdbHLH104-GFP*, *MdSIZ1-MYC*, and *antiMdSIZ1* were under the control of the *35S* promoter. Subsequently, the resultant vectors were genetically transformed into apple calli and Arabidopsis (*Arabidopsis thaliana*) plants with the *Agrobacterium tumefaciens* strains LBA4404 and GV3101, as described by Horsch et al. (1985).

*Agrobacterium rhizogenes*-mediated transformation was performed as described by Xiao et al. (2014) with minor modifications. In brief, a 350-bp fragment of *MdSIZ1* (1,197–1,546 bp) was inserted into the pK7GWIWG2(II)-RedRoot vector under control of the 35S promoter using Gateway cloning technology to construct the RNA interference (RNAi) transformation vector. The following primer pairs were used: asMdSIZ1-F/asMdSIZ1-R for 350-bp fragment of *MdSIZ1* and RNAi-MdSIZ1-F/RNAi-MdSIZ1-R for the fragment used for Gateway cloning (Supplemental Table S1). The resultant vector, harboring a 35S:DsRED1 cassette to overexpress the DsRED fluorescent protein, was introduced into *A. rhizogenes* MSU440 with the help of the pRiA4 plasmid and then used for transient transformation.

Subsequently, 3-week-old 'Gala' apple tissue cultures were cut off a part of the stem and then immersed in *A. rhizogenes* MSU440 solution ($OD_{600}$ = 0.6–0.8) for 15 min. Inoculated plants were then transferred to 1/2 MS medium containing 300 mg/L cefotaxime at 25°C for hairy-root induction. Examination of transgenic hairy roots for DsRED1 fluorescence was performed using a fluorescence microscope (AX10; Carl Zeiss) employing the DsRED filter set (excitation, 546/12 nm; emission, 605/75 nm). As a result of preliminary tests, nontransformed hairy roots lacking DsRED fluorescence were cut off, and the transformed chimera plants were then used for follow-up experiments.

### Gene Expression Analysis

Total RNA was isolated from apple plants, hairy roots, calli, and Arabidopsis plants using an OmniPlant RNA Kit (DNase I; Cwbiotech), following the manufacturer's instructions. First-strand cDNA was synthesized using a PrimeScript first-strand cDNA synthesis kit (Takara), following the manufacturer's instructions.

Subsequently, cDNA was diluted to 2.5 ng $\mu L^{-1}$ with $ddH_2O$ for RT-qPCR, and the reactions were performed using the UltraSYBR Mixture (with ROX I; Cwbiotech) in a reaction volume of 20 μL. The following primer pairs were used: QS-F/QS-R for *MdSIZ1*, Q104-F/Q104-R for *MdbHLH104*, Q105-F/Q105-R for *MdbHLH105*, QI-F/QI-R for *MdIRT1*, QF-F/QF-R for *MdFRO2*, QA1-F/QA1-R for *MdAHA1*, QA3-F/QA3-R for *MdAHA3*, QA7-F/QA7-R for *MdAHA7*, QA8-F/QA8-R for *MdAHA8*, QA9-F/QA9-R for *MdAHA9*, QA11-F/QA11-R for *MdAHA11*, and QA12-F/QA12-R for *MdAHA12* (Supplemental Table S2). *Md18S* and *MdActin* were used as internal controls.

### Y2H Assay

Yeast (*Saccharomyces cerevisiae*) two-hybrid assays (Y2H) were performed as described by Zhou et al. (2017). In brief, full-length cDNAs of MdSCE1, MdbHLH104, MdbHLH105, MdbHLH115, MdbHLH11, MdbHLH121, MdPYE, MdAHA1, MdAHA3, MdAHA7, MdAHA8, MdAHA9, MdAHA11, and MdAHA12 were inserted into pGAD424 (Clontech) to generate an in-frame fusion with the GAL4 activation domain. The primer pairs used for gene cloning are listed in Supplemental Table S1. The domain-deleted form (1–427 aa) of MdSIZ1 was excised by *Sma*I and *Pst*I double digestion and cloned into pGBT9 to generate an in-frame fusion with the GAL4 DNA-binding domain. Full-length MdSIZ1 was self-activated in β-galactosidase assays in yeast. All of the constructs were transformed into the Y2H strain using the lithium acetate method. Subsequently, yeast cells were plated onto selective medium lacking Trp and Leu (−Trp/−Leu), and the colonies were then cultured in YPDA liquid medium consisting of 2% (w/v) Bacto Pepton, 1% (w/v) yeast extract, 2% (w/v) Glc, and 1% (v/v) 100× adenine until $OD_{600}$ reached 0.25. Next, the solution was diluted 10 times, 100 times, and 1,000 times in turn, dropped on the selective medium lacking Trp and Leu (−Trp/−Leu) or lacking Trp, Leu, His, and Adenine (−Leu/−Trp/−His/−Ade), and grown for 2 d at 28°C.

### Pull-Down Assays

These assays were performed as described by Zhou et al. (2017). The *MdbHLH104* coding sequence was amplified using the primer pair MdbHLH104-F/MdbHLH104-R (Supplemental Table S1) and excised by *Bam*HI and *Sal*I double digestion and then cloned into the *PGEX-4T-1* vector for GST-tag fusion. The full-length cDNA of *MdSIZ1* was amplified using the primer pair MdSIZ1-F/MdSIZ1-R (Supplemental Table S1) and cloned into the *pEASY-Blunt E1* expression vector using original TA cloning kit (Transgene) for His-tag fusion. Then, both proteins were individually expressed in and purified from *Escherichia coli* BL21 (DE3). Subsequently, recombinant GST-MdbHLH104 fusion and His-MdSIZ1 fusion proteins were mixed in equal volumes, and following incubation, were purified with a GST column. The pellet fraction was then detected via immunoblotting using an anti-His antibody (Abmart).

### Co-IP Assay

For Co-IP assays, MdbHLH104-GFP and GFP proteins were IPed from the *35S:MdbHLH104-GFP* and *35S:GFP* (pBIN) transgenic apple plants with

anti-GFP antibodies (Abmart) using the Pierce classic IP kit (Thermo Fisher), following the manufacturer's instructions. MdbHLH104-GFP proteins and GFP proteins in whole-cell lysates (Input) and MdSIZ1 proteins in the pellet fraction (IP) were detected via immunoblot analysis with anti-GFP and anti-MdSIZ1 antibodies (customized by Abmart), respectively.

## Sumoylation Assays

Sumoylation assays were performed in vivo as described by Zhou et al. (2017). In brief, 6 μg of GST-MdbHLH104, GST-MdbHLH104$^{K139R}$, GST-MdbHLH104$^{K153R}$, and GST-MdbHLH104$^{K139R/K153R}$ were incubated with 0.5 μg of recombinant human SAE1 protein (product code, ab96772), 0.5 μg of SAE2/UBA2 peptide (product code, ab109093), 2 μg of human UBE2I/UBC9 peptide (product code: ab30701), 5 μg of recombinant human SUMO1 protein (product code, ab3801; Abcam), and with or without 8 μg of His-MdSIZ1 for 1.5 h at 37°C. Sumoylated proteins were double detected with anti-SUMO1 (Abcam) and anti-GST antibodies (Abmart), respectively.

For in vivo sumoylation assays, the 28-d-old *MdbHLH104-GFP* transgenic apple plants and 2-week-old transgenic calli overexpressing the *MdbHLH104-GFP*, *MdbHLH104-GFP/MdSIZ1-MYC*, *MdbHLH104-GFP/antiMdSIZ1*, or *MdbHLH104$^{K139R/K153R}$-GFP* fusions were treated in Fe-deficient conditions for 1 h before total proteins were immunoprecipitated with anti-GFP antibodies using a Pierce classic IP kit (Thermo Fisher), following the manufacturer's instructions. Western blot analyses were subsequently performed with anti-GFP (Abmart) or anti-SUMO1 (Abmart) antibodies.

## Protein Degradation Assays

For in vivo degradation assays, after pretreatment in Fe-deficient conditions for 1 h, 2-week-old *MdbHLH104-GFP*, *MdbHLH104-GFP/MdSIZ1-MYC*, *MdbHLH104$^{K139R/K153R}$-GFP*, and *MdbHLH104$^{K139R/K153R}$-GFP/MdSIZ1-MYC* transgenic calli were placed in Fe-sufficient liquid medium containing 250 μM cycloheximide translational inhibitor for different durations and sampled simultaneously to detect MdbHLH104-GFP protein abundance using an anti-GFP antibody. For MG132 (26S proteasome inhibitor) treatment, the Fe deficiency pretreated transgenic calli were treated with 50 μM MG132 for 6 h and then used for the protein degradation assay. DMSO was used as a negative control for MG132. The protein concentrations were quantified using Quantity One 1-D Analysis Software (Bio-Rad).

## In Vivo Ubiquitination Assays

For the in vivo ubiquitination assays, the Fe deficiency pretreated transgenic calli overexpressing *MdbHLH104-GFP*, *MdbHLH104-GFP/MdSIZ1-MYC*, and *MdbHLH104$^{K139R/K153R}$-GFP* were treated with 50 μM MG132 for 6 h and then treated with Fe-sufficient conditions for 6 h or not. Then, MdbHLH104-GFP proteins were IPed using an anti-GFP antibody using the Pierce classic IP kit (Thermo Fisher), following the manufacturer's instructions. MdbHLH104-GFP proteins in whole-cell lysates prior to treatment (Input) and in the pellet fraction (IP), or ubiquitinated MdbHLH104 proteins in the pellet fraction (IP), were detected via immunoblot analysis with anti-GFP and antiubiquitin antibodies (Sigma-Aldrich, Germany), respectively.

## Viral Vector-Based Transformation Analysis

To generate antisense viral expression vectors, the *MdbHLH104* fragment was amplified using the primer pair asMdbHLH104-F/asMdbHLH104-R (Supplemental Table S1) and excised by *Eco*RI and *Kpn*I double digestion and then cloned into the *tobacco rattle virus* (TRV) vector in the antisense orientation under the control of the dual *35S* promoter. The resultant vectors were then transiently transformed into *MdSIZ1-MYC* transgenic calli using the *Agrobacterium tumefaciens* strain LBA4404 with the auxiliary vector *TRV1*. The empty vector *TRV2* was used as a negative control.

## PM H$^+$-ATPase H$^+$-Transport Activity Assays

PM H$^+$-ATPases were isolated as described by Zhao et al. (2016a). The apple calli were grown on Fe-sufficient normal media and then transferred to the media at a pH of 6 or 8 for 5 d for PM H$^+$-ATPase H$^+$-transport activity detection. For *Agrobacterium tumefaciens*-infected apple plants, the plants with transgenic roots were grown on sand with the addition of Hoagland's solution of pH 6 for 1 month and then transferred to the sand with the addition of Hoagland's solution of pH 6 or pH 8 for 7 d for PM H$^+$-ATPase H$^+$-transport activity detection. For Arabidopsis, the 14-d-old seedlings grown on normal (pH 6) or alkaline (pH 8) media were used. PMs were isolated with a buffer consisting of 15 mM Tris-Cl (pH 7.5), 0.5 M Suc, 1 mM EGTA, 1 mM EDTA, 6% (w/v) polyvinylpyrrolidone, 0.1% (w/v) bovine serum albumin, 0.1 mM dithiothreitol, and 1 mM phenylmethylsulfonyl fluoride. Microsomal pellets were obtained from the homogenate as described by Zhao et al. (2016a). All steps were performed at 4°C or on ice. Subsequently, an inside-acid pH gradient (ΔpH), which was formed in the vesicles by the activity of the H$^+$-ATPase, was measured as a decrease (quench) in the fluorescence of quinacrine (a pH-sensitive fluorescent probe), which has been described in detail by Zhao et al. (2016a). Specific PM H$^+$-ATPase H$^+$-transport activity was calculated by dividing the change in fluorescence by the mass of PM protein in the reaction per unit time (ΔF/min per mg of protein).

## GUS Analysis

Histochemical staining to detect GUS activity and quantitative analysis of GUS in apple calli was performed as described by Xie et al. (2012).

For histochemical staining, the transgenic calli were immersed in GUS staining buffer (1 mM 5-bromo-4-chloro-3-indolyl-β-GlcA solution in 100 mM sodium phosphate, pH 7.0, 0.1 mM EDTA, 0.5 mM ferrocyanide, 0.5 mM ferricyanide, and 0.1% [v/v] Triton X-100) at 37°C for 1 h. After staining, the calli were photographed.

For the quantitative analysis of GUS activity, the proteins were extracted with 1 mL of extraction buffer (50 mM $NaHPO_4$, pH 7.0, 10 mM β-mercaptoethanol, 10 mM $Na_2$ EDTA, 0.1% (v/v) Triton X-100) and 1 mL RIPA Lysis buffer (Beyotime) from the transgenic apple calli. The concentration of total protein was determined with the Protein Assay kit (Bio-Rad). One hundred milliliters of the extract was then added to 900 μL of GUS reaction buffer containing 1 mM 4-methylumbelliferone glucuronide, and the mixture was incubated at 37°C. After the reaction proceeded for 0, 5, 10, 15, 30, and 60 min, 100 μL of the reaction mixture was added to 900 μL of the stop solution (1 M sodium carbonate). The fluorescence was measured using a Versa Flour Spectrofluorometer at an excitation wavelength of 365 nm and an emission wavelength of 450 nm.

## Chlorophyll Content Measurement

The *Agrobacterium tumefaciens*-infected apple plants were grown on sand with the addition of Hoagland solution of pH 6 for 1 month and then transferred to the sand with the addition of Hoagland solution of pH 6 or pH 8 for 20 d. Subsequently, the young leaves were collected and ground into powder in liquid nitrogen to measure chlorophyll content. The powder was then resuspended in 80% (v/v) acetone and centrifuged at 10,000*g* for 5 min. Chlorophyll concentrations were calculated as described by Zhao et al. (2016a). For Arabidopsis, the 14-d-old seedlings grown on normal (pH 6) or alkaline (pH 8) media were used.

## Rhizosphere Acidification Assay

Acidification assays were performed as described by Yi et al. (1994) and Zhao et al. (2016a). The apple calli were grown on normal medium (pH 6) for 14 d, transferred to alkaline medium (pH 8) for 5 d, and then transferred to 1% (w/v) agar plates containing 0.006% (w/v) bromocresol purple and 0.2 mM $CaSO_4$ (pH 6.0–6.5) for 36 h for phenotype analysis.

For *Agrobacterium tumefaciens*-infected apple plants, the plants were grown on sand with the addition of Hoagland solution of pH 6 for 1 month and then transferred to the sand with the addition of Hoagland solution of pH 6 or pH 8 for 7 d. Subsequently, the plants were transferred to a 1% (w/v) agar plate containing 0.006% (w/v) bromocresol purple and 0.2 mM $CaSO_4$ (pH 6.0–6.5) for 36 h for phenotype analysis.

For Arabidopsis, seeds were germinated on normal (pH 6) or alkaline medium (pH 8) for 14 d. Subsequently, three plants of every line were transferred to bromocresol purple agar plates, as mentioned above, for 36 h for phenotype analysis.

## Ferrous Staining Assay

The apple calli were grown on normal medium (pH 6) for 14 d and then transferred to alkaline medium (pH 8) for 5 d. Subsequently, the calli were transferred to liquid MS media containing 300 μM Ferrozine for 12 h for

ferrous staining. Ferrozine reagent forms a red-colored complex with ferrous iron, but not with ferric iron, and the Fe(II) is trapped by Ferrozine to produce a red product (Stookey, 1970).

For quantification of ferrous complex formed by ferrozine, the optical density of the complex was measured at 562 nm wavelength. At this wavelength, the molar absorptivity is 27,900 (Stookey, 1970), and the concentration of the complex was calculated according to Lambert-Beer law.

## Fe Concentration Measurement

Fe content measurements were carried out as described by Kobayashi et al. (2013). The apple calli were grown on Fe-sufficient normal media and then transferred to the media at a pH of 6 or 8 for 5 d for Fe content measurement. For *Agrobacterium tumefaciens*-infected apple plants, the plants with transgenic roots were grown on sand with the addition of Hoagland's solution of pH 6 for 1 month and then transferred to the sand with the addition of Hoagland solution of pH 6 or pH 8 for 20 d for Fe content measurement. For Arabidopsis, the 14-d-old seedlings grown on normal (pH 6) or alkaline (pH 8) media were used. Apple calli, plants, and Arabidopsis plants were dried for 1 to 2 d at 80°C and then wet-ashed with $HNO_3$ and $H_2O_2$ for 60 min at 220°C using a muffle furnace. Fe content analysis was performed using inductively coupled plasma spectroscopy.

## Accession Numbers

Sequence data from this article can be found in the Genome Database for Rosacea (GDR) under accession numbers MdSIZ1 (MDP0000125173), MdSCE1 (MDP0000465760), MdbHLH104 (MDP0000825749), MdbHLH105 (MDP0000264803), MdbHLH115 (MDP0000323291), MdbHLH11 (MDP0000275635), MdbHLH121 (MDP0000494181), MdPYE (MDP0000301871), MdAHA1 (MDP0000136397), MdAHA3 (MDP0000150049), MdAHA7 (MDP0000162032), MdAHA8 (MDP0000181085), MdAHA9 (MDP0000195785), MdAHA11 (MDP0000249645), MdAHA12 (MDP0000259837), MdFRO2 (MDP0000226559), and MdIRT1 (MDP0000940721).

## Supplemental materials

The following supplemental materials are available.

**Supplemental Figure S1**. MdSIZ1 is an important protein in the response to Fe deficiency in apple

**Supplemental Figure S2**. The transcript levels of *MdSIZ1* were inhibited in transgenic hair roots of *MdSIZ1*-RNAi chimeric plants

**Supplemental Figure S3**. MdSIZ1 promotes PM $H^+$-ATPase-mediated acidification capacity and Fe acquisition in apple calli

**Supplemental Figure S4**. MdSIZ1 specifically interacts with MdbHLH104 in yeast cells

**Supplemental Figure S5**. Potential sumoylation site consensus sequences predicted in MdbHLH104 proteins

**Supplemental Figure S6**. Identification of transgenic apple calli

**Supplemental Figure S7**. The transcript levels of *MdbHLH104* were not influenced by MdSIZ1

**Supplemental Figure S8**. Interactions among MdSIZ1 and 7 MdAHA proteins

**Supplemental Figure S9**. The transcript levels of *MdbHLH38* and *MdbHLH39* were up-regulated by MdbHLH104 and MdSIZ1

**Supplemental Figure S10**. The expression levels of *MdSCE1*

**Supplemental Table S1**. Primers used for gene cloning

**Supplemental Table S2**. Primers used for RT-qPCR

## ACKNOWLEDGMENTS

This work was supported by grants from the National Natural Science Foundation of China (31430074 and 31772275), the Ministry of Education of China (IRT15R42), the Ministry of Agriculture of China (CARS-28) and Shandong Province (SDAIT-06-03).

Received March 6, 2018; accepted October 9, 2018; published October 17, 2018.

## LITERATURE CITED

**Briat JF, Dubos C, Gaymard F** (2015) Iron nutrition, biomass production, and plant product quality. Trends Plant Sci **20**: 33–40

**Catala R, Ouyang J, Abreu IA, Hu Y, Seo H, Zhang X, Chua NH** (2007) The Arabidopsis E3 SUMO ligase SIZ1 regulates plant growth and drought responses. Plant Cell **19**: 2952–2966

**Colangelo EP, Guerinot ML** (2004) The essential basic helix-loop-helix protein FIT1 is required for the iron deficiency response. Plant Cell **16**: 3400–3412

**Curie C, Briat JF** (2003) Iron transport and signaling in plants. Annu Rev Plant Biol **54**: 183–206

**Dalir N, Khoshgoftarmanesh AH, Massah A, Shariatmadari H** (2017) Plasma membrane ATPase and $H^+$ transport activities of microsomal membranes from wheat roots under Ni deficiency conditions as affected by exogenous histidine. Environ Exp Bot **135**: 56–62

**de Souza Pinto S, de Souza AE, Oliva MA, Pereira EG** (2016) Oxidative damage and photosynthetic impairment in tropical rice cultivars upon exposure to excess iron. Sci Agric **73**: 217–226

**Flotho A, Melchior F** (2013) Sumoylation: a regulatory protein modification in health and disease. Annu Rev Biochem **82**: 357–385

**Fuglsang AT, Guo Y, Cuin TA, Qiu Q, Song C, Kristiansen KA, Bych K, Schulz A, Shabala S, Schumaker KS, Palmgren MG, Zhu JK** (2007) Arabidopsis protein kinase PKS5 inhibits the plasma membrane $H^+$ -ATPase by preventing interaction with 14-3-3 protein. Plant Cell **19**: 1617–1634

**Gill G** (2004) SUMO and ubiquitin in the nucleus: different functions, similar mechanisms? Genes Dev **18**: 2046–2059

**Guo CL, Chen Q, Zhao XL, Chen XQ, Zhao Y, Wang L, Li KZ, Yu YX, Chen LM** (2013) Al-enhanced expression and interaction of 14-3-3 protein and plasma membrane $H^+$-ATPase is related to Al-induced citrate secretion in an Al-resistant black soybean. Plant Mol Biol Report **31**: 1012–1024

**Hänsch R, Mendel RR** (2009) Physiological functions of mineral micronutrients (Cu, Zn, Mn, Fe, Ni, Mo, B, Cl). Curr Opin Plant Biol **12**: 259–266

**Haruta M, Sussman MR** (2012) The effect of a genetically reduced plasma membrane protonmotive force on vegetative growth of Arabidopsis. Plant Physiol **158**: 1158–1171

**Hell R, Stephan UW** (2003) Iron uptake, trafficking and homeostasis in plants. Planta **216**: 541–551

**Hindt MN, Guerinot ML** (2012) Getting a sense for signals: regulation of the plant iron deficiency response. Biochim Biophys Acta **1823**: 1521–1530

**Hoagland DR, Arnon DI** (1950) The water-culture method for growing plants without soil. California Agricultural Experiment Station Circular, Vol. **347**: College of Agriculture, University of California, Berkerely, Berekeley, CA, pp 1–38

**Horsch R, Fry J, Hoffmann N, Eichholtz D** (1985) A simple and general method for transferring genes into plants. Science **227**: 1229–1231 17757866

**Huang L, Yang S, Zhang S, Liu M, Lai J, Qi Y, Shi S, Wang J, Wang Y, Xie Q, Yang C** (2009) The Arabidopsis SUMO E3 ligase AtMMS21, a homologue of NSE2/MMS21, regulates cell proliferation in the root. Plant J **60**: 666–678

**Ishida T, Yoshimura M, Miura K, Sugimoto K** (2012) MMS21/HPY2 and SIZ1, two Arabidopsis SUMO E3 ligases, have distinct functions in development. PLoS One **7**: e46897

**Kim HS, Oh JM, Luan S, Carlson JE, Ahn SJ** (2013) Cold stress causes rapid but differential changes in properties of plasma membrane H(+)-ATPase of camelina and rapeseed. J Plant Physiol **170**: 828–837

**Kobayashi T, Nishizawa NK** (2012) Iron uptake, translocation, and regulation in higher plants. Annu Rev Plant Biol **63**: 131–152

**Kobayashi T, Nakanishi H, Nishizawa NK** (2010) Recent insights into iron homeostasis and their application in graminaceous crops. Proc Jpn Acad, Ser B, Phys Biol Sci **86**: 900–913

**Kobayashi T, Nagasaka S, Senoura T, Itai RN, Nakanishi H, Nishizawa NK** (2013) Iron-binding haemerythrin RING ubiquitin ligases regulate plant iron responses and accumulation. Nat Commun **4**: 2792

**Leivar P, Monte E, Al-Sady B, Carle C, Storer A, Alonso JM, Ecker JR, Quail PH** (2008) The Arabidopsis phytochrome-interacting factor PIF7, together with PIF3 and PIF4, regulates responses to prolonged red light by modulating phyB levels. Plant Cell **20**: 337–352

**Li X, Zhang H, Ai Q, Liang G, Yu D** (2016) Two bHLH transcription factors, bHLH34 and bHLH104, regulate iron homeostasis in Arabidopsis thaliana. Plant Physiol **170**: 2478–2493

**Li YY, Mao K, Zhao C, Zhao XY, Zhang HL, Shu HR, Hao YJ** (2012) MdCOP1 ubiquitin E3 ligases interact with MdMYB1 to regulate light-induced anthocyanin biosynthesis and red fruit coloration in apple. Plant Physiol **160**: 1011–1022 22855936

**Li Z, Hu Q, Zhou M, Vandenbrink J, Li D, Menchyk N, Reighard S, Norris A, Liu H, Sun D, Luo H** (2013) Heterologous expression of OsSIZ1, a rice SUMO E3 ligase, enhances broad abiotic stress tolerance in transgenic creeping bentgrass. Plant Biotechnol J **11**: 432–445

**Lin XL, Niu D, Hu ZL, Kim DH, Jin YH, Cai B, Liu P, Miura K, Yun DJ, Kim WY, Lin R, Jin JB** (2016) An Arabidopsis SUMO E3 ligase, SIZ1, negatively regulates photomorphogenesis by promoting COP1 activity. PLoS Genet **12**: e1006016

**Ling HQ, Bauer P, Bereczky Z, Keller B, Ganal M** (2002) The tomato fer gene encoding a bHLH protein controls iron-uptake responses in roots. Proc Natl Acad Sci USA **99**: 13938–13943

**Long TA, Tsukagoshi H, Busch W, Lahner B, Salt DE, Benfey PN** (2010) The bHLH transcription factor POPEYE regulates response to iron deficiency in Arabidopsis roots. Plant Cell **22**: 2219–2236

**Mandadi KK, Misra A, Ren S, McKnight TD** (2009) BT2, a BTB protein, mediates multiple responses to nutrients, stresses, and hormones in Arabidopsis. Plant Physiol **150**: 1930–1939

**Miura K, Rus A, Sharkhuu A, Yokoi S, Karthikeyan AS, Raghothama KG, Baek D, Koo YD, Jin JB, Bressan RA, Yun DJ, Hasegawa PM** (2005) The Arabidopsis SUMO E3 ligase SIZ1 controls phosphate deficiency responses. Proc Natl Acad Sci USA **102**: 7760–7765

**Miura K, Jin JB, Lee J, Yoo CY, Stirm V, Miura T, Ashworth EN, Bressan RA, Yun DJ, Hasegawa PM** (2007) SIZ1-mediated sumoylation of ICE1 controls CBF3/DREB1A expression and freezing tolerance in Arabidopsis. Plant Cell **19**: 1403–1414

**Miura K, Lee J, Jin JB, Yoo CY, Miura T, Hasegawa PM** (2009) Sumoylation of ABI5 by the Arabidopsis SUMO E3 ligase SIZ1 negatively regulates abscisic acid signaling. Proc Natl Acad Sci USA **106**: 5418–5423

**Mori S** (1999) Iron acquisition by plants. Curr Opin Plant Biol **2**: 250–253

**Novatchkova M, Tomanov K, Hofmann K, Stuible HP, Bachmair A** (2012) Update on sumoylation: defining core components of the plant SUMO conjugation system by phylogenetic comparison. New Phytol **195**: 23–31

**Palmgren MG** (2001) Plant plasma membrane H+-ATPases: powerhouses for nutrient uptake. Annu Rev Plant Physiol Plant Mol Biol **52**: 817–845 11337417

**Park BS, Song JT, Seo HS** (2011) Arabidopsis nitrate reductase activity is stimulated by the E3 SUMO ligase AtSIZ1. Nat Commun **2**: 400

**Sampson DA, Wang M, Matunis MJ** (2001) The small ubiquitin-like modifier-1 (SUMO-1) consensus sequence mediates Ubc9 binding and is essential for SUMO-1 modification. J Biol Chem **276**: 21664–21669

**Santi S, Schmidt W** (2009) Dissecting iron deficiency-induced proton extrusion in Arabidopsis roots. New Phytol **183**: 1072–1084

**Selote D, Samira R, Matthiadis A, Gillikin JW, Long TA** (2015) Iron-binding E3 ligase mediates iron response in plants by targeting basic helix-loop-helix transcription factors. Plant Physiol **167**: 273–286

**Shen H, He LF, Sasaki T, Yamamoto Y, Zheng SJ, Ligaba A, Yan XL, Ahn SJ, Yamaguchi M, Sasakawa H, Matsumoto H** (2005) Citrate secretion coupled with the modulation of soybean root tip under aluminum stress. Up-regulation of transcription, translation, and threonine-oriented phosphorylation of plasma membrane $H^+$-ATPase. Plant Physiol **138**: 287–296

**Sibole JV, Cabot C, Michalke W, Poschenrieder C, Barceló J** (2005) Relationship between expression of the PM $H^+$-ATPase, growth and ion partitioning in the leaves of salt-treated Medicago species. Planta **221**: 557–566

**Spartz AK, Ren H, Park MY, Grandt KN, Lee SH, Murphy AS, Sussman MR, Overvoorde PJ, Gray WM** (2014) SAUR inhibition of PP2C-D phosphatases activates plasma membrane $H^+$-ATPases to promote cell expansion in Arabidopsis. Plant Cell **26**: 2129–2142

**Stookey LL** (1970) Ferrozine—a new spectrophotometric reagent for iron. Anal Chem **42**: 779–781

**Ulrich HD** (2005) Mutual interactions between the SUMO and ubiquitin systems: a plea of no contest. Trends Cell Biol **15**: 525–532

**Walker EL, Connolly EL** (2008) Time to pump iron: iron-deficiency-signaling mechanisms of higher plants. Curr Opin Plant Biol **11**: 530–535

**Wang N, Cui Y, Liu Y, Fan H, Du J, Huang Z, Yuan Y, Wu H, Ling HQ** (2013) Requirement and functional redundancy of Ib subgroup bHLH proteins for iron deficiency responses and uptake in *Arabidopsis thaliana*. Mol Plant **6**: 503–513

**Xiao X, Ma F, Chen CL, Guo WW** (2014) High efficient transformation of auxin reporter gene into trifoliate orange via Agrobacterium rhizogenes-mediated co-transformation. Plant Cell Tissue Organ Cult **118**: 137–146

**Xie XB, Li S, Zhang RF, Zhao J, Chen YC, Zhao Q, Yao YX, You CX, Zhang XS, Hao YJ** (2012) The bHLH transcription factor MdbHLH3 promotes anthocyanin accumulation and fruit colouration in response to low temperature in apples. Plant Cell Environ **35**: 1884–1897

**Yang D, Chen D, Wang P, Jiang D, Xu H, Pang X, Chen L, Yu Y, Li K** (2016) Aluminium-inhibited $NO_3^-$ uptake is related to Al-increased $H_2O_2$ content and Al-decreased plasma membrane ATPase activity in the root tips of Al-sensitive black soybean. Funct Plant Biol **44**: 198–207

**Yi Y, Saleeba JA, Guerinot ML** (1994) Iron uptake in *Arabidopsis thaliana*. *In* **J Manthey, DE Crowley, DG Luster**, eds, Biochemistry of Metal Micronutrients in the Rhizosphere.Lewis Publishers, Boca Raton, FL, pp 295–307

**Yu Y, Duan X, Ding X, Chen C, Zhu D, Yin K, Cao L, Song X, Zhu P, Li Q, Nisa ZU, Yu J,** (2017) A novel AP2/ERF family transcription factor from Glycine soja, GsERF71, is a DNA binding protein that positively regulates alkaline stress tolerance in Arabidopsis. Plant Mol Biol **94**: 509–530

**Yuan KH** (2005) Fit indices versus test statistics. Multivariate Behav Res **40**: 115–148

**Yuan W, Zhang D, Song T, Xu F, Lin S, Xu W, Li Q, Zhu Y, Liang J, Zhang J** (2017) Arabidopsis plasma membrane $H^+$-ATPase genes AHA2 and AHA7 have distinct and overlapping roles in the modulation of root tip $H^+$ efflux in response to low-phosphorus stress. J Exp Bot **68**: 1731–1741

**Yuan Y, Wu H, Wang N, Li J, Zhao W, Du J, Wang D, Ling HQ** (2008) FIT interacts with AtbHLH38 and AtbHLH39 in regulating iron uptake gene expression for iron homeostasis in Arabidopsis. Cell Res **18**: 385–397

**Zhang J, Liu B, Li M, Feng D, Jin H, Wang P, Liu J, Xiong F, Wang J, Wang HB** (2015) The bHLH transcription factor bHLH104 interacts with IAA-LEUCINE RESISTANT3 and modulates iron homeostasis in Arabidopsis. Plant Cell **27**: 787–805

**Zhao M, Song A, Li P, Chen S, Jiang J, Chen F** (2014) A bHLH transcription factor regulates iron intake under Fe deficiency in chrysanthemum. Sci Rep **4**: 6694

**Zhao Q, Ren YR, Wang QJ, Yao YX, You CX, Hao YJ** (2016a) Overexpression of MdbHLH104 gene enhances the tolerance to iron deficiency in apple. Plant Biotechnol J **14**: 1633–1645

**Zhao Q, Ren YR, Wang QJ, Wang XF, You CX, Hao YJ** (2016b) Ubiquitination-related MdBT scaffold proteins target a bHLH transcription factor for iron homeostasis. Plant Physiol **172**: 1973–1988

**Zheng Y, Schumaker KS, Guo Y** (2012) Sumoylation of transcription factor MYB30 by the small ubiquitin-like modifier E3 ligase SIZ1 mediates abscisic acid response in Arabidopsis thaliana. Proc Natl Acad Sci USA **109**: 12822–12827

**Zhou LJ, Li YY, Zhang RF, Zhang CL, Xie XB, Zhao C, Hao YJ** (2017) The small ubiquitin-like modifier E3 ligase MdSIZ1 promotes anthocyanin accumulation by sumoylating MdMYB1 under low-temperature conditions in apple. Plant Cell Environ **40**: 2068–2080